HAL open science

Environmental DNA reveals a mismatch between diversity facets of Amazonian fishes in response to contrasting geographical, environmental and anthropogenic effects

Opale Coutant, Céline Jézéquel, Karel Mokany, Isabel Cantera, Raphaël Covain, Alice Valentini, Tony Dejean, Sébastien Brosse, Jérôme Murienne

To cite this version:

Opale Coutant, Céline Jézéquel, Karel Mokany, Isabel Cantera, Raphaël Covain, et al.. Environmental DNA reveals a mismatch between diversity facets of Amazonian fishes in response to contrasting geographical, environmental and anthropogenic effects. Global Change Biology, 2023, 29 (7), pp.1741-1758. 10.1111/gcb.16533 . hal-04060932

HAL Id: hal-04060932

https://hal.science/hal-04060932v1

Submitted on 6 Apr 2023

HAL is a multi-disciplinary open access archive for the deposit and dissemination of scientific research documents, whether they are published or not. The documents may come from teaching and research institutions in France or abroad, or from public or private research centers.

L'archive ouverte pluridisciplinaire **HAL**, est destinée au dépôt et à la diffusion de documents scientifiques de niveau recherche, publiés ou non, émanant des établissements d'enseignement et de recherche français ou étrangers, des laboratoires publics ou privés.

Distributed under a Creative Commons Attribution 4.0 International License

Check for updates

Received: 23 August 2022 | Accepted: 13 November 2022

DOI: 10.1111/gcb.16533

Global Change Biology WILEY

RESEARCH ARTICLE

Environmental DNA reveals a mismatch between diversity facets of Amazonian fishes in response to contrasting geographical, environmental and anthropogenic effects

Opale Coutant[1] | Céline Jézéquel[1] | Karel Mokany[2] | Isabel Cantera[3] | Raphaël Covain[4] | Alice Valentini[5] | Tony Dejean[5] | Sébastien Brosse[1] | Jérôme Murienne[1]

[1]Laboratoire Evolution et Diversité Biologique (UMR 5174), CNRS, IRD, Université Paul Sabatier, Toulouse, France

[2]CSIRO, Canberra, Australian Capital Territory, Australia

[3]Department of Environmental Science and Policy, Università degli Studi di Milano, Milano, Italy

[4]Department of Herpetology and Ichthyology, Museum of Natural History, Geneva, Switzerland

[5]SPYGEN, Le Bourget-du-Lac, France

Correspondence
Opale Coutant, Laboratoire Evolution et Diversité Biologique (UMR 5174), CNRS, IRD, Université Paul Sabatier, 118 route de Narbonne, Toulouse 31062, France.
Email: opale.coutant@univ-tlse3.fr

Funding information
Agence Nationale de la Recherche, Grant/Award Number: ANR-10-LABX-0041, ANR-10-LABX-25-01, ANR-11-LABX-0010 and ANR-17-CE02-0007-01

Abstract

Freshwater ecosystems are among the most endangered ecosystem in the world. Understanding how human activities affect these ecosystems requires disentangling and quantifying the contribution of the factors driving community assembly. While it has been largely studied in temperate freshwaters, tropical ecosystems remain challenging to study due to the high species richness and the lack of knowledge on species distribution. Here, the use of eDNA-based fish inventories combined to a community-level modelling approach allowed depicting of assembly rules and quantifying the relative contribution of geographic, environmental and anthropic factors to fish assembly. We then used the model predictions to map spatial biodiversity and assess the representativity of sites surveyed in French Guiana within the EU Water Framework Directive (WFD) and highlighted areas that should host unique freshwater fish assemblages. We demonstrated a mismatch between the taxonomic and functional diversity. Taxonomic assemblages between but also within basins were mainly the results of dispersal limitation resulting from basin isolation and natural river barriers. Contrastingly, functional assemblages were ruled by environmental and anthropic factors. The regional mapping of fish diversity indicated that the sites surveyed within the EU WFD had a better representativity of the regional functional diversity than taxonomic diversity. Importantly, we also showed that the assemblages expected to be the most altered by anthropic factors were the most poorly represented in terms of functional diversity in the surveyed sites. The predictions of unique functional and taxonomic assemblages could, therefore, guide the establishment of new survey sites to increase fish diversity representativity and improve this monitoring program.

KEYWORDS
β-diversity, community modelling, deforestation, environmental DNA, freshwater fish, functional diversity, taxonomic diversity

Sébastien Brosse and Jérôme Murienne should be considered as joint senior authors.

This is an open access article under the terms of the Creative Commons Attribution License, which permits use, distribution and reproduction in any medium, provided the original work is properly cited.
© 2022 The Authors. *Global Change Biology* published by John Wiley & Sons Ltd.

1 | INTRODUCTION

While accounting for less than 1% of the earth's surface, freshwaters harbour more than 6% of the described species (Dudgeon et al., 2006). For instance, 17,000 fish species inhabit freshwaters and account for 25% of all vertebrates (van der Laan, 2020). Yet, freshwaters are also among the most imperilled ecosystems on earth, with more than 50% of the world's rivers experiencing human-mediated biodiversity declines (Su et al., 2021), threatening more than 22% of the freshwater fish species across the globe (Albert et al., 2021).

Both local environmental factors (at the habitat scale) and large-scale variables (e.g. climate, land cover) are recognized as natural determinants of fish species assemblages (Benone et al., 2020; López-Delgado et al., 2020). At a large spatial scale, freshwater fish distributions are mostly determined by the historical connections among basins during the quaternary low-sea-level period, promoting the dispersal of species between basins (Carvajal-Quintero et al., 2019). Within basins, freshwater ecosystems are characterized by a dendritic network structure in which hydrologic connectivity dictates a dispersal pathway from upstream to downstream (Vannote et al., 1980). This dispersal pathway has been recognized as a major driver of freshwater fish distribution, generating a distribution pattern reported in the river continuum concept, which predicts an increase in species richness from upstream to downstream (Harvey et al., 2018; Vannote et al., 1980). Freshwater fish distribution is thus mediated by multiple environmental factors operating at different spatial scales (Benone et al., 2020). This distribution pattern is determined by a combination of biotic and abiotic factors including species dispersal capacities, physical characteristics of the river such as dispersal barriers (e.g. rapids or waterfalls) or habitat hosting capacity and diversity (e.g. upstream parts are smaller than downstream parts), which all vary longitudinally along the network (Carvajal-Quintero et al., 2019). Moreover, the two spatial major drivers that are positioned in the river network and historical connections between river basins suggest that connectivity is a crucial parameter of freshwater fish distribution (Carvajal-Quintero et al., 2019; Harvey et al., 2018). Besides natural determinants, anthropic activities can also determine fish biodiversity patterns, especially in highly connected ecosystems, where altering habitat connectivity and quality modify ecological processes and patterns. For instance, Zeni et al. (2019) demonstrated that deforestation led to biotic homogenization of stream habitats, which was responsible for an increased functional redundancy in fish assemblages across tropical regions of the globe. Freshwaters are deeply impacted by global changes but often remain at the edge of the discussions (Albert et al., 2021). Yet, these ecosystems are strongly tied to human well-being as they provide multiple essential ecosystem services including the maintenance of hydro-climatic regimes, human food, energy production, transportation, recreation, as well as waste disposal and remediation (Albert et al., 2021; van Rees et al., 2021). Consequently, quantifying the relative role of natural (historical and environmental) and anthropogenic factors in structuring biodiversity distribution is pivotal to design adequate conservation strategies.

Measuring the contribution of historical, environmental and anthropic factors in freshwater fish assembly rules requires understanding how processes shaping diversity apply and vary from local to regional scales (Socolar et al., 2016). This question can be addressed by measuring community dissimilarity between sites within a region (β-diversity), which can reveal the spatial structure of biodiversity (Whittaker, 1960) and predict changes in biodiversity over the entire region (γ-diversity) from local biodiversity changes (α-diversity) (Socolar et al., 2016). β-diversity approaches have frequently been conducted on the taxonomic facet of biodiversity, treating all the species as functionally equivalent (Roa-Fuentes et al., 2019). However, taxonomy alone is not sufficient to understand community assembly while multi-faceted assessments of biodiversity provide complementary views on the different processes acting on communities (Roa-Fuentes et al., 2019; Villéger et al., 2013). In fact, taxonomic and functional facets can disclose mismatch patterns. For example, a pair of assemblages exhibiting taxonomic differentiation can show a low relative functional β-diversity if the species from each assemblage are functionally equivalent (Villéger et al., 2013). This has significant conservation implications because biodiversity facets may respond differently to environmental pressures and across scales (Devictor et al., 2010).

The environmental DNA (eDNA) metabarcoding method (Taberlet et al., 2012) enables rapid and efficient biodiversity inventories at multiple sites. It has been proven particularly efficient for fast biodiversity assessments in species-rich tropical rivers, where traditional fish survey methods, be they observational or capture-based, are time-consuming, can be invasive and/or of limited efficiency (Cantera et al., 2019; Dickie et al., 2018; Lear et al., 2018; Shu et al., 2020). To date, the use of eDNA-based inventories to map biodiversity at large scales (e.g. catchment scale for freshwater fish) remains scarce, probably because efforts have been so far directed towards the development and optimization of robust eDNA metabarcoding protocols (Coutant et al., 2020). Recently, eDNA has nevertheless been proved efficient in delineating conservation areas within whole river catchments over a 200,000 km^2 territory (Blackman et al., 2021). It has also been used to develop a hydrology-based modelling framework revealing the spatial patterns of aquatic insects over an entire river catchment (Carraro et al., 2020).

Here, using the information on fish distribution over three river basins of French Guiana, we investigated the structuration of fish taxonomic and functional diversity and questioned whether different processes drive these two biodiversity facets. We hypothesized that (1) geographical processes mainly drive regional fish taxonomic facet while we expect that (2) fish functional facet is mostly governed by local environmental and anthropic factors. The regional taxonomic diversity should therefore root in the historical connections between basins while the functional diversity should be shaped by the regional variations of environmental and anthropic factors. To answer these research questions, we used eDNA-based inventories from 85 sites located along three rivers (Maroni, Sinnamary and Oyapock). These rivers are considered among the most preserved areas worldwide (Su et al., 2021) but are facing an unprecedented rise of threats linked to deforestation and gold mining, altering water physicochemical properties and generating strong disturbances to aquatic biodiversity (Cantera, Coutant, et al., 2022; Castello

13652486, 2023, 7, Downloaded from https://onlinelibrary.wiley.com/doi/10.1111/gcb.16533 by Cochrane France, Wiley Online Library on [06/04/2023]. See the Terms and Conditions (https://onlinelibrary.wiley.com/terms-and-conditions) on Wiley Online Library for rules of use; OA articles are governed by the applicable Creative Commons License

et al., 2013). In addition, as unravelling the assembly rules and spatial patterns of taxonomic and functional diversity will constitute a benchmark for developing conservation strategies in such high biodiversity regions, we used generalized dissimilarity models (GDMs) to map and predict β-diversity over seven river basins from French Guiana, extending over 112,000 km (Maroni, Oyapock, Sinnamary, Mana, Comté, Kourou and Approuague rivers). We then asked the extent to which the sites surveyed in French Guiana within the EU Water Framework Directive (WFD) are representative of the biodiversity encountered in the entire region and highlighted areas that should host unique freshwater fish assemblages.

2 | MATERIAL AND METHOD

2.1 | Study area

Sampling was conducted on three river basins of the Guiana Shield, in the north-eastern Amazonian biome (Figure 1). Altogether, the three basins cover a surface of 101,365 km^2. The Maroni River is 612 km long from its source to its estuary, and its basin covers a surface of ±68,000 km^2 in Suriname and French Guiana. The Oyapock River (length, 404 km; area, 26,800 km^2) is located in the state of Amapa in Brazil and French Guiana. The Sinnamary River (length, 262 km; area, 6565 km^2) is situated within the territory of French Guiana. The climate of the entire study area is relatively homogeneous and the region is covered by dense, uniform lowland primary rainforest. The altitude is in the range of 0–860 m a.s.l. The regional climate is equatorial, and the annual rainfall ranges from 2000 mm in the south-west to 3600 mm in the northeast. These rivers face different levels of anthropogenic pressure, unevenly distributed along the watercourses. The Maroni river is the most inhabited with *c*. 83,000 habitants (INSEE, 2020) unevenly distributed from Saint-Laurent du Maroni to Pidima village, which constitutes the most upstream human settlement on the Maroni river (Figure 1). The Maroni river is also the most affected by human activities, mainly legal and illegal gold mining, which represented 8058 ha of deforestation (0.37% of the catchment area in 2014) spanning from Saint-Laurent du Maroni to upstream of Maripasoula (Gallay et al., 2018). Only the most upstream part of the Maroni River (upstream from Pidima,

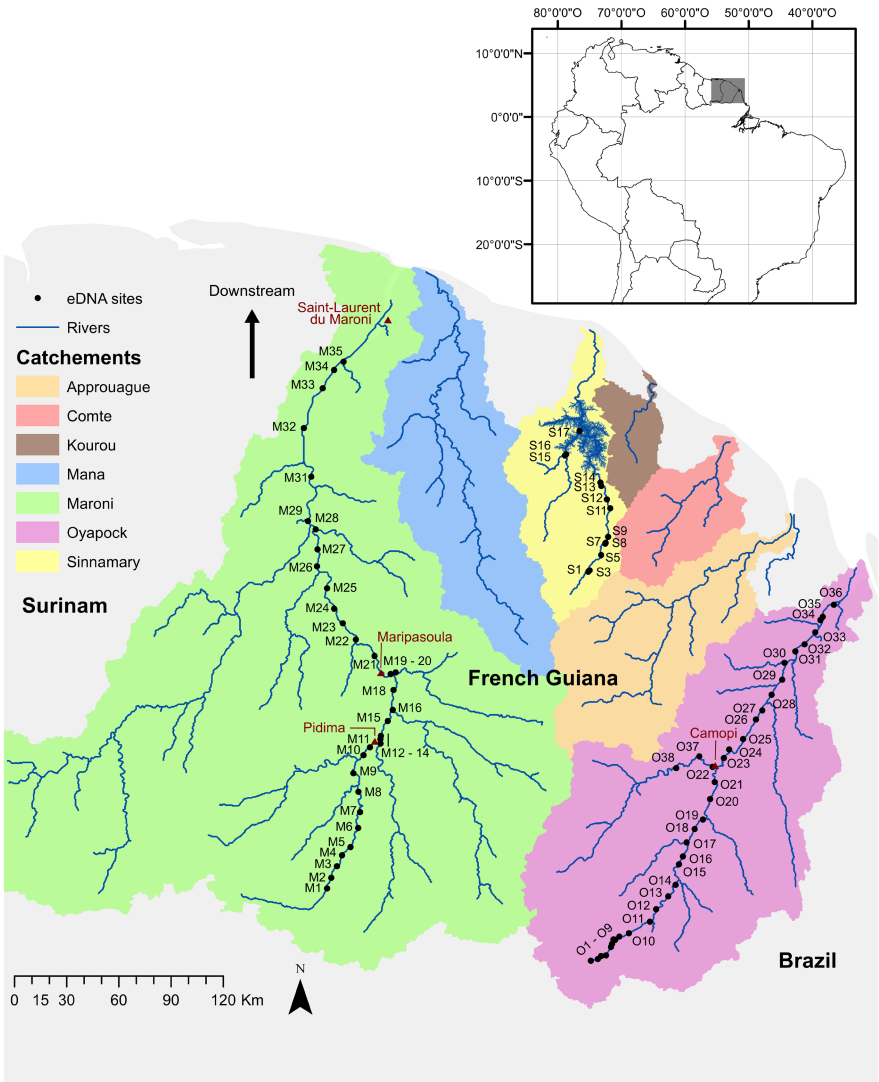

FIGURE 1 Map of the study area and the 85 biodiversity sampling sites. The inset map on the right indicates the location of the study area in South America in grey.

13652486, 2023, 7, Downloaded from https://onlinelibrary.wiley.com/doi/10.1111/gcb.16533 by Cochrane France, Wiley Online Library on [06/04/2023]. See the Terms and Conditions (https://onlinelibrary.wiley.com/terms-and-conditions) on Wiley Online Library for rules of use; OA articles are governed by the applicable Creative Commons License

Figure 1) has not been impacted by human activities. The Oyapock River is more preserved, with only three villages and *c.* 6000 habitants (INSEE, 2020). Gold mining is much less developed than in the Maroni basin and represented 1547 ha of deforestation in 2014 (0.06% of the catchment area), mainly concentrated near the village of Camopi (Gallay et al., 2018). The Sinnamary River is not exploited for gold, but the building of a large hydroelectric dam (Petit Saut dam) in 1994–1995 has severely modified the landscape: 365 km^2 of primary rainforest were flooded, leaving hundreds of islands of various sizes covering a total area of 105 km^2 (Vié, 1999). Several human settlements are located downstream from the dam, while the upstream part of the river remains free from human settlements, with only occasional recreational fishing.

2.2 | Fish sampling

2.2.1 | Water sampling

Environmental DNA was collected from water samples at 85 locations (hereafter, sites) along the main channel and the large tributaries of the Maroni, Oyapock and Sinnamary rivers (Figure 1). All the metadata associated with the samples are described in Murienne et al. (2019) and available on the CEBA geoportal (http://vmcebagn-dev.ird.fr) and in Table S1. At all sites, the river was wider than 20 m and deeper than 1 m (Strahler orders 4–7; Figure S2). At all rivers, the sites were sequentially sampled from downstream to upstream. Following the protocol of Cantera et al. (2019), we collected the eDNA by filtering two replicates during 30 min and resulting approximately in 30 L of water per site. A peristaltic pump (Vampire Sampler; Buerkle GmbH) and single-use tubing were used to pump the water into a single-use filtration capsule (VigiDNA, 0.45 μm; SPYGEN). The tubing input was placed a few centimetres below the water surface in zones with high water flow, as recommended by Cilleros et al. (2019). Sampling was performed in turbulent areas to ensure optimal eDNA homogeneity throughout the water column. To avoid eDNA cross-contamination among sites, the operator remained on emerging rocks downstream from the filtration area. At the end of filtration, the capsule was emptied, filled with 80 mL CL1 conservation buffer (SPYGEN) and stored in the dark for up to 1 month before the DNA extraction.

2.2.2 | eDNA laboratory and bioinformatics

For the DNA extraction, each filtration capsule was agitated on an S50 shaker (Ingenieurbüro CAT M. Zipperer GmbH) at 800 rpm for 15 min, decanted into a 50 ml tube and centrifuged at 15,000 *g* and 6°C for 15 min. The supernatant was removed with a sterile pipette, leaving 15 ml of liquid at the bottom of the tube. Subsequently, 33 ml of ethanol and 1.5 ml of 3 M sodium acetate were added to each 50 ml tube and the mixtures were stored at −20°C for at least one night. The tubes were then centrifuged at 15,000×*g* and 6°C for 15 min, and the supernatants were discarded. Then, 720 μl of ATL buffer from a DNeasy Blood & Tissue Extraction Kit (Qiagen) was added. The tubes were vortexed and the supernatants were transferred to 2 ml tubes containing 20 μl Proteinase K (Macherey-Nagel GmbH). The tubes were then incubated at 56°C for 2 h. DNA extraction was performed using a NucleoSpin Soil kit (Macherey-Nagel GmbH) starting from step six of the manufacturer's instructions. Elution was performed by adding 100 μl of SE buffer twice. After the DNA extraction, the samples were tested for inhibition by qPCR following the protocol of Biggs et al. (2015). Briefly, quantitative PCRs were performed in duplicate for each sample. If at least one of the replicates showed a different Ct (Cycle threshold) than expected (at least 2 Cts), the sample was considered inhibited and diluted fivefold before the amplification.

We used the 'teleo' primer pair (Valentini et al., 2016) (forward: 3′-ACACCGCCCGTCACTCT-5′; reverse: 3′-CTTCCGGTACACTTACCATG-5′) which targets a 60 bp marker located at the 5′ end of the 12S ribosomal gene, a region presenting a high variability across fish species. The performance of the 'teleo' primer pair has been investigated by Polanco et al. (2021), who showed that it can efficiently discriminate fish species of the Maroni River, the river with the highest species richness in French Guiana. The 'teleo' primer has thus been used in previous studies focused on French Guianese fish fauna (Cantera, Coutant, et al., 2022; Cantera, Decotte, et al., 2022; Cantera et al., 2019; Cilleros et al., 2019). The DNA amplifications were performed in a final volume of 25 μl containing 1 U AmpliTaq Gold DNA Polymerase (Applied Biosystems), 0.2 μM of each primer, 10 mM Tris-HCl, 50 mM KCl, 2.5 mM $MgCl_2$, 0.2 mM of each dNTP and 3 μl DNA template. Human blocking primer was added to the mixture for the 'teleo' primers (Valentini et al., 2016) (5′-ACCCTCCTCAAGTATACTTCAAAGGAC-C3-3′) at final concentrations of 4 μM and 0.2 μg/μl bovine serum albumin (BSA; Roche Diagnostics). Twelve PCR replicates were performed per field sample (85 sites × 2 field replicates × 12 PCR replicates, 2040 PCR replicates in total). The forward and reverse primer tags were identical within each PCR replicate. The PCR mixture was denatured at 95°C for 10 min, followed by 50 cycles of 30 s at 95°C, 30 s at 55°C and 1 min at 72°C and a final elongation step at 72°C for 7 min. This step was conducted in a dedicated room for DNA amplification that is kept under negative air pressure. The success of the amplification was verified using capillary electrophoresis (QIAxcel; Qiagen GmbH) and the samples were purified using a MinElute PCR purification kit (Qiagen GmbH). Before sequencing, purified PCR products were quantified using capillary electrophoresis and then pooled in equal volumes to achieve an expected sequencing depth of 500,000 reads per sample before DNA library preparation.

For the fish analyses, 10 libraries were prepared using a PCR-free library protocol (https://www.fasteris.com/metafast) at Fasteris, Geneva, Switzerland. Four libraries were sequenced on an Illumina HiSeq 2500 (2 × 125 bp) (Illumina) with a HiSeq SBS Kit v4 (Illumina), three were sequenced on a MiSeq (2 × 125 bp) (Illumina) with a MiSeq Flow Cell Kit Version 3 (Illumina), and three libraries were sequenced on a NextSeq (2 × 150 bp + 8) (Illumina) with a NextSeq

13652486, 2023, 7, Downloaded from https://onlinelibrary.wiley.com/doi/10.1111/gcb.16533 by Cochrane France, Wiley Online Library on [06/04/2023]. See the Terms and Conditions (https://onlinelibrary.wiley.com/terms-and-conditions) on Wiley Online Library for rules of use; OA articles are governed by the applicable Creative Commons License

Mid kit (Illumina). The libraries run on the NextSeq were equally distributed in four lanes. Sequencing was performed according to the manufacturer's instructions at Fasteris.

The sequence reads were analyzed with the OBITools (Boyer et al., 2016) according to the protocol described by Valentini et al. (2016). Briefly, the forward and reverse reads were assembled with the `illuminapairedend` programme. The `ngsfilter` programme was then used to assign the sequences to each sample. A separate dataset was created for each sample by splitting the original dataset into several files with `obisplit`. Sequences shorter than 20 bp or occurring less than 10 times per sample were discarded. Sequences labelled by the `obiclean` programme as 'internal' and probably corresponding to PCR errors were also discarded. The `ecotag` programme was used for taxonomic assignment of molecular operational taxonomic units (MOTUs). An updated version of the reference database from Cilleros et al. (2019) was used. This database is a local database of French Guianese freshwater fish referencing the 12S mtDNA fragments of 367 species, representing 92% of the 400 freshwater fish species described in French Guiana. Among these referenced species, 9 (2.5%) cannot be discriminated at the species level with the 'teleo' primer pair. For the 33 (8%) species missing in the database, we were not able to collect DNA. The GenBank nucleotide database was consulted, but it contained little information on the Guianese fish species. Most of the sequences were derived from Cilleros et al. (2019). Species-level assignments were validated only for ≥98% sequence identity with the reference database. Sequences below this threshold were discarded. We discarded all MOTUs with a frequency of occurrence below 0.001 per library in each sample, considered as tag-jumps (Schnell et al., 2015). These thresholds were empirically determined to clear all reads from the extraction and PCR negative controls included in our global data production procedure as suggested by De Barba et al. (2014) and Taberlet et al. (2018). For the samples sequenced on a NextSeq platform, only species present in at least two lanes were kept. These bioinformatic analyses provided a species-by-site matrix with read number per species (Table S2).

2.3 | Predictor variables

2.3.1 | Environmental and anthropogenic variables

Satellite-based environmental variables (n = 41) were extracted from the Near Global Freshwater-specific Environmental variables for biodiversity analyses at 1 km resolution (Domisch et al., 2015). When there was no data available at the location of the sampling sites, the nearest pixel value was assigned. In addition, four water hydro-chemical parameters measured in the field for each site were used: conductivity, water temperature, pH and turbidity (Table S3).

For anthropogenic variables, we quantified deforestation using the Global Forest Change database (Hansen et al., 2013). This dataset identifies areas deforested between 2001 and 2017 at a 30 m spatial scale. To incorporate deforested areas before 2000, tree canopy cover data for that year were also used. Except for river courses, all pixels with <25% canopy closure were regarded as deforested. Finally, surfaces deforested by gold mining activity in French Guiana, Suriname and Northern Brazil were also included (Rahm et al., 2017). We merged those datasets to create an integrative disturbance variable that quantifies the deforestation around the sampling sites. Here, deforestation intensity around each eDNA sampling site is considered an integrative measure of human-mediated environmental disturbances including gold mining, logging, agriculture and human settlements (Cantera, Coutant, et al., 2022).

We calculated the mean percentage of deforestation upstream (along the sub-basin drainage network) and upstream and downstream of the sampling sites (Table S3; Figure S1). Indeed, we previously showed that 30 km represented the most relevant upstream spatial extent to investigate biodiversity responses to deforestation in our system (Cantera, Coutant, et al., 2022). We considered the sites' upstream sub-basin drainage network areas to account for the hydrologic connectivity of rivers and the associated water-mediated downstream transfer of matters and pollutants. We also considered circular areas around sampling sites because it integrates the hydrologic connectivity of rivers but also the potential influence of downstream impacts on sampling sites (Figure S1). We delineated sub-basins by applying a Flow Accumulation algorithm to the SRTM Global 30 m Model Elevation (Becker et al., 2009). Then, for each sampling site, we quantified deforestation intensity by summing upstream or upstream and downstream deforested surfaces and dividing this sum by the area of the delineated spatial extent to obtain percentages of deforestation (Figure S1).

2.3.2 | Geographical effect

Three pairwise distance variables were computed: (i) the Euclidean distances; (ii) the site distances following the actual riverine dendritic network and (iii) the paleo-distances between sites, which are the distances following the river network from the last glacial maximum (−20,000 years) when the sea level was at −120 m. This allowed accounting for connections between basins that no longer exist.

For the actual and the paleo-distances, the distances between different basins were calculated following the coastline. Distances were calculated in ArcGIS, using the network analyst extension and the OD cost matrix function. The distance matrices were used as input in a non-metric multidimensional scaling (NMDS) analysis to transform the matrices into coordinates on a two-dimensional space. The coordinates obtained through NMDS were then used to calculate Euclidean distances in GDMs (see Section 2.4.3).

2.3.3 | Predictor spatialization

We spatialized the predictors using a 1 km spatial resolution to be consistent with the spatial scale of the inventories. We previously

13652486, 2023, 7, Downloaded from https://onlinelibrary.wiley.com/doi/10.1111/gcb.16533 by Cochrane France, Wiley Online Library on [06/04/2023]. See the Terms and Conditions (https://onlinelibrary.wiley.com/terms-and-conditions) on Wiley Online Library for rules of use; OA articles are governed by the applicable Creative Commons License

demonstrated that eDNA does not represent an integrative measure of biodiversity across the whole upstream river basin, but provides a relevant picture of local fish assemblages (Cantera, Decotte, et al., 2022). We first modelled the hydrographic network by applying a Flow Accumulation algorithm to the SRTM Global 1 km Model Elevation using the ArcHydro tools from ArcGis. Spatialization was conducted with different procedures depending on the variables: geographic distance, field variables, environmental variables or anthropic variables. For geographic distance, we calculated the pairwise paleo-distances between all pairs of pixels and implemented these distances in an NMDS to compute NMDS-based coordinates. For field variables, we interpolated the data along the hydrographic network using the inverse distance weighting method. The anthropic variable was spatialized using the same methods as for sampling sites. Considering each pixel of the SRTM Global 1 km Model Elevation as outlets, we delineated 30-km upstream sub-basin areas by applying a Flow Accumulation algorithm to the SRTM Global 1 km Model Elevation. We then calculated percentages of deforestation for each pixel within the delineated areas (upstream areas or upstream–downstream areas) (Table S3, Figure S1). Environmental data from the Near Global Freshwater Environmental variables were already provided at a 1-km resolution; therefore, we only modified the hydrographic network to consider the same network as the one used for anthropic and field variables (considering only the streams with Strahler order from 4 to 7, Figure S2).

2.4 | Response variables

2.4.1 | Taxonomic β-diversity

We calculated fish taxonomic β-diversity based on the Jaccard's dissimilarity coefficient using the *formatsitepair* function of the GDM package (Fitzpatrick et al., 2022). Using the Baselga framework implemented in the beta-part package (Baselga & Orme, 2012), we also computed the turnover (β_{jtu}) and nestedness (β_{jne}) contribution to taxonomic β-diversity (β_{jac}) to understand if β-diversity is mostly the results of difference in species compositions between sites (Baselga, 2010; Carvalho et al., 2012). Disentangling the underlying processes of β-diversity delivers fundamental insights into the mechanisms shaping communities. For instance, if β-diversity results from spatial turnover, it may signify that environmental sorting and/or geographical constraints govern fish assembly (Qian et al., 2005).

2.4.2 | Functional β-diversity

Morphological and ecological traits were used to functionally characterize each fish species. For the morphological traits, 12 measurements were made using side-view pictures of mature fish to compute 10 unitless ratios (hereafter, traits) reflecting food acquisition and locomotion strategies (Villéger et al., 2017) (Table S4). The morphological traits were measured for as many individuals as possible (1–28 depending on the species), and the averages of all measurements per species were used. For the ecological traits, six qualitative traits related to trophy, behaviour and habitat preference were selected and collected from FishBase (http://www.fishbase.org) and the literature (Table S4). Morphological and ecological traits were missing for 18 species (6.7% of the considered fish). For these species, we assigned the average values of the morphological measures and the ecological traits of the closest related species. Using these fish functional, morphological and ecological attributes, we calculated a species dissimilarity matrix using the Gower's distance, which can handle mixed data of numeric and class variables while standardizing them. We then implemented the dissimilarity matrix into a multidimensional space using a principal coordinate analysis (PCoA) and applying the Cailliez correction (Cailliez, 1983) for negative eigenvalues to build a functional space. This analysis provides coordinates for all the species in a global functional space (Table S5). We retained the four first PCoA axes, which was the best compromise to maximize functional space quality and minimize data loss (to compute site functional β-diversity, sites must possess a higher number of species than the number of selected axes, Maire et al., 2015). Using species coordinates, we finally calculated a site functional β-diversity (β_{jac}) matrix and partitioned it into turnover (β_{jtu}) and nestedness (β_{jtu}) matrices based on the Jaccard dissimilarity coefficient. These analyses were realized with the betapart package, with the functions *functional.beta.core* to create a betapart object and *functional.beta.pair* to compute the matrices.

2.4.3 | Generalised dissimilarity modelling

GDM is a method that relates the dissimilarities of a response variable with ecological distances (Ferrier et al., 2007). It is based on the regression of a dissimilarity matrix and accommodates nonlinearities often encountered in ecological datasets using I-spline coefficients (monotonic cubic splines function) for each explanatory variable. Higher coefficients indicate higher rates of change of the response variable along the gradient of a given explanatory variable. Nonlinearities occur for two reasons: (i) there is a curvilinear relationship between ecological separation and compositional dissimilarity because most dissimilarity metrics range from 0 to 1. Therefore, once no species are shared between sites, the dissimilarity value takes on an asymptotic value of 1 while the ecological separation keeps increasing. (ii) There is a variation in the rate of compositional changes along ecological gradients.

2.4.4 | Variable selection

The GDMs implemented with the paleo-distances had the highest explanatory power. Thus, this distance measure was used as a geographic proxy in all the GDMs (see Table S6 for model comparisons with the three different geographic measures).

To obtain the most relevant predictors, we gathered many predictor variables from different databases (Table S3). Because they provided redundant information in certain cases, we conducted a

13652486, 2023, 7, Downloaded from https://onlinelibrary.wiley.com/doi/10.1111/gcb.16533 by Cochrane France, Wiley Online Library on [06/04/2023]. See the Terms and Conditions (https://onlinelibrary.wiley.com/terms-and-conditions) on Wiley Online Library for rules of use; OA articles are governed by the applicable Creative Commons License

preliminary analysis following a variable selection protocol using the collinearity diagnostic variance inflation factor. We used the *vifstep* function from the USDM package (Naimi, 2015), which excludes the highly correlated variables from the set through a stepwise procedure. We built two sets of predictors, each including one of the two anthropic variables (30 km upstream deforested areas or 30-km upstream and downstream deforested areas). This step removed 27 satellite-based environmental variables from the initial set. Fifteen satellite-based variables and five field variables were kept for further analyses. Table S7 shows the selected variables, and Table S8 contains the two different sets of used predictors. The two sets were not identical because correlation coefficients between anthropic and environmental variables changed depending on the spatial extent considered.

2.4.5 | Generalised dissimilarity model implementation

GDMs were fitted using the gdm package (Fitzpatrick et al., 2022). For each biodiversity facet (taxonomic and functional) and β-diversity and its turnover component, we first formatted the data using the *formatsitepair* function. We then ran GDMs using the *gdm.varImp* function (one model for each set of predictors), including the site paleo-distances as the geographic variable (see Section 4). We did not run GDMs with the nestedness component because nestedness was too low and the models did not converge. We used the three I-spline basis function and the significance of each model was calculated by matrix permutation, by comparing the deviance explained by the original model with the distributions of the deviance calculated to all permutations while conducting a backward elimination process to select the best predictors. The selection of the best set of predictors for each biodiversity facet was performed by choosing the model minimizing the deviance and maximizing the percentage of deviance explained (Table S8). Then, the best predictors within the selected set were retained only if they were significant and explained more than 1% of the deviance (percentage of deviance explained by each variable is determined by summing the coefficients of the I-splines from the GDM). Table S9 shows the model results with the two sets of predictors for each biodiversity facet. Deviance partitioning was used to calculate the unique and shared contributions of the best-selected set of environmental, anthropic and geographic variables, using the function *gdm.partition.deviance* of the gdm package.

2.5 | Taxonomic and functional predictions of β-diversity

We predicted β-diversity and turnover over seven rivers (from west to east: Maroni, Mana, Approuague, Sinnamary, Kourou, Comte and Oyapock, see Figure 1) from the best GDMs. Predictions were only computed for the main tributaries as only fish communities sampled on stream orders of 4–7 were considered (Figure S2). To generate spatially explicit GDM predictions, the *gdm.transform* function from the gdm package was first used to create layers embodying the parameters of the fitted models. More precisely, the spline functions computed for each predictor from the fitted GDMs were applied to spatialised predictors covering the seven rivers to create transformed layers displaying how β-diversity varies in space according to historical, environmental and anthropic variables. Then, the GDM-transformed layers were used to assess the fish representativeness of sites currently surveyed since 2000 within the EU WFD (Water Framework Directive 2000, https://ec.europa.eu/environment/water/water-framework/index_en.html). We calculated the predicted average similarity of each location (each 1 km raster pixel) to a set of 27 sites where fish communities are monitored every year as part of WFD. Additionally, we computed the uniqueness of each location (each 1 km raster pixel) by calculating the mean similarity between each location and all the locations across the region. These two analyses were conducted following Mokany et al. (2022).

3 | RESULTS

3.1 | Taxonomic and functional β-diversity between and within basins

In the 85 eDNA sampling sites, 235 fish species were detected with site species richness ranging from 20 to 134 species (median = 68). The fish species belonged to 13 orders, 42 families and 139 genera.

3.1.1 | Inter-basin β-diversity

The mean functional β-diversity was significantly lower than that of taxonomic β-diversity (Mann–Whitney *U*-rank test, $U = 4{,}994{,}284$, $p < .001$, $n = 2248$, Figure 2a; Table 1) and the mean functional turnover was significantly lower than that of taxonomic turnover (Mann–Whitney *U*-rank test, $U = 5{,}050{,}823$, $p < .001$, $n = 2248$, Figure 2b; Table 1). Contrastingly, the mean functional nestedness was significantly greater than that of taxonomic nestedness (Mann–Whitney *U*-rank test, $U = 1{,}072{,}523$, $p < .001$, $n = 2248$, Figure 2c; Table 1). On the one hand, the contribution of taxonomic nestedness to β-diversity was low and β-diversity was mainly driven by taxonomic turnover (Mann–Whitney *U*-rank test, $U = 5{,}053{,}465$, $p < .001$, $n = 2248$) (Figure 2a–c; Table 1). On the other hand, functional turnover contributed slightly more to functional β-diversity than functional nestedness (Mann–Whitney *U*-rank test, $U = 3{,}011{,}049$, $p < .001$, $n = 2248$), but both components jointly shaped functional β_{jac} (Figure 2a–c; Table 1).

3.1.2 | Intra-basin β-diversity

The mean functional β-diversity was significantly lower than that of taxonomic β-diversity (Mann–Whitney *U*-rank test, $U = 1{,}389{,}066$,

13652486, 2023, 7, Downloaded from https://onlinelibrary.wiley.com/doi/10.1111/gcb.16533 by Cochrane France, Wiley Online Library on [06/04/2023]. See the Terms and Conditions (https://onlinelibrary.wiley.com/terms-and-conditions) on Wiley Online Library for rules of use; OA articles are governed by the applicable Creative Commons License

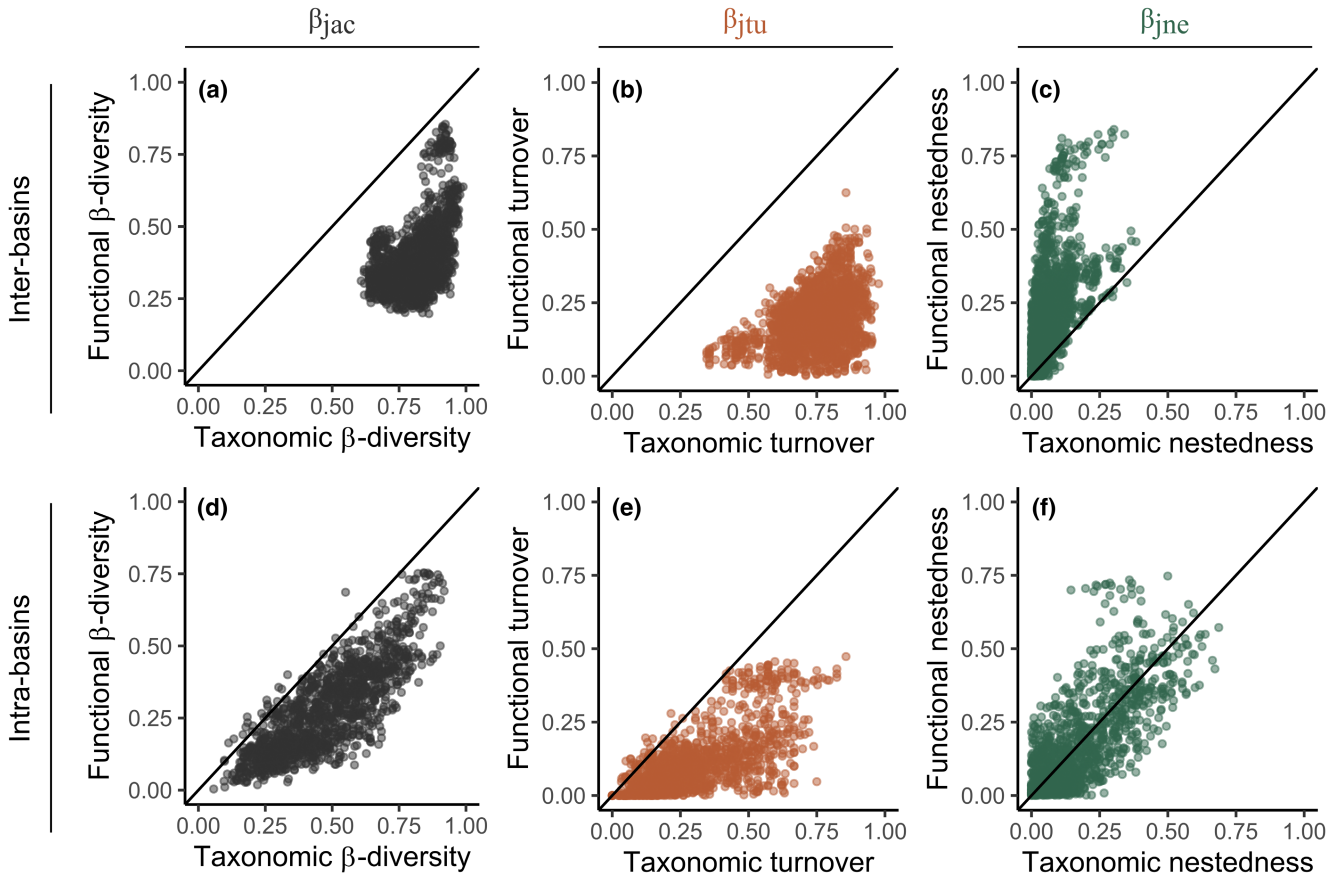

FIGURE 2 Relationships between taxonomic and functional β-diversity (β_{jac}) and its turnover (β_{jtu}) and nestedness (β_{ne}) components for pairwise comparisons of fish assemblages. (a–c) Inter-basin comparisons, (d–f) intra-basin comparisons.

TABLE 1 Mean ± SD taxonomic and functional values for pairwise combinations of sites located in different basins (inter-basin β-diversity) and for pairwise combinations of sites located within the same basins (intra-basin β-diversity)

	Taxonomic			Functional		
	β-diversity	Turnover	Nestedness	β-diversity	Turnover	Nestedness
Inter-basin β-diversity	0.81 ± 0.08	0.75 ± 0.11	0.06 ± 0.06	0.37 ± 0.11	0.19 ± 0.09	0.18 ± 0.16
Intra-basin β-diversity	0.48 ± 0.18	0.31 ± 0.18	0.17 ± 0.14	0.28 ± 0.15	0.11 ± 0.11	0.17 ± 0.16

$p < .001$, n = 1322, Figure 2e; Table 1) and the mean functional turnover was significantly lower to that of taxonomic turnover (Mann–Whitney U-rank test, U = 1,475,102, $p < .001$, n = 1322, Figure 2f; Table 1). The mean taxonomic nestedness was slightly greater than that of the functional nestedness (Mann–Whitney U-rank test, U = 920,404, $p < .02$, n = 1322, Figure 2g; Table 1). Overall, taxonomic turnover contributed significantly more to taxonomic β-diversity than taxonomic nestedness (Mann–Whitney U-rank test, U = 1,288,227, $p < .001$, n = 1322; Figure 2d–f; Table 1). Functional nestedness contributed significantly more to functional β-diversity than functional turnover (Mann–++Whitney U-rank test, U = 723,161, $p < .001$, n = 1322; Figure 2d–f; Table 1).

3.2 | Drivers of taxonomic and functional fish diversity

For all the GDMs, the paleo-distances between sites was the best geographic proxy. For the taxonomic β-diversity, the GDM with the highest explanatory power was the model considering deforestation over a 30 km upstream sub-basin area. This model explained 84.4% of the total deviance in β-diversity (Table S10). The most important predictor was the geographic distance; its sole effect explained 54.4% of the deviance. The two environmental predictors (elevation range and water temperature) explained together 5.9% of the deviance, while the anthropic variable only accounted for 3.3% of

13652486, 2023, 7, Downloaded from https://onlinelibrary.wiley.com/doi/10.1111/gcb.16533 by Cochrane France, Wiley Online Library on [06/04/2023]. See the Terms and Conditions (https://onlinelibrary.wiley.com/terms-and-conditions) on Wiley Online Library for rules of use; OA articles are governed by the applicable Creative Commons License

the deviance (Figure 3a). Taxonomic β-diversity increased with site paleo-distances and was maximal between the most distant sites (Figure 4a). It also steadily increased with site difference in water temperature and exhibited an abrupt increase with a site elevation range between 600 and 800 m (Figure 4b,c). Finally, taxonomic β-diversity consistently increased along the site deforestation gradient, with maximal values of β-diversity reached between the less and most deforested sites (Figure 4d).

For the taxonomic turnover, the GDM with the highest explanatory power was the model considering deforestation over a 30-km

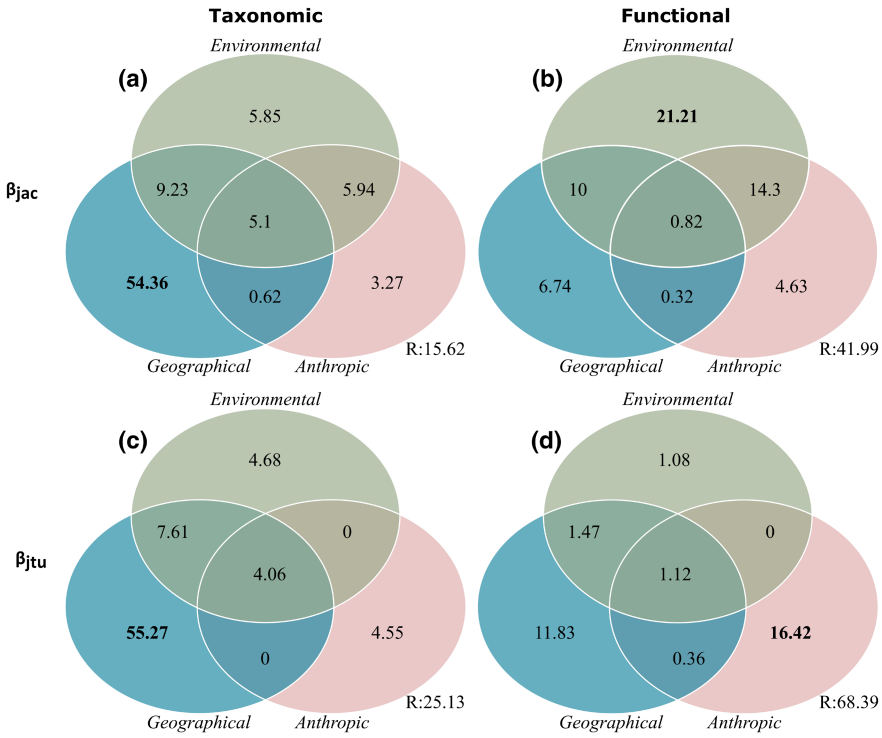

FIGURE 3 Partitioning of generalized dissimilarity model deviance of fish taxonomic and functional β-diversity (β_{jac}) and turnover (β_{jtu}) into geographical (blue), environmental (green) and anthropic (pink) variables across the 85 sampling sites. GDM deviance partitioning for (a) taxonomic β-diversity, (b) functional β-diversity, (c) the turnover component of taxonomic β-diversity, (d) the turnover component of functional β-diversity. Values represent percentages of deviance explained. Venn diagrams represent the unique and shared contribution of each variable. R refers to the model residual deviance (unexplained deviance). Bold values display the variables with the highest contributions.

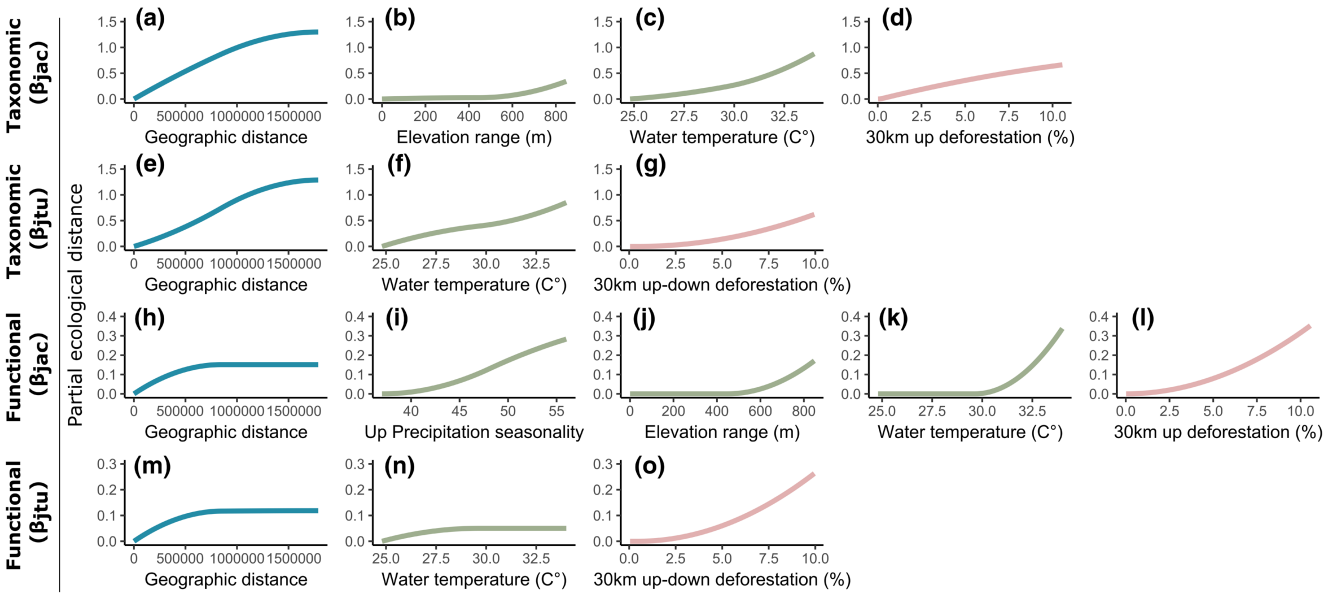

FIGURE 4 I-splines generated for geographical (blue), environmental (green) and anthropic (pink) variables from the final generalized dissimilarity models (Table S10). I-splines from the final GDMs for (a–d) taxonomic β-diversity, (e–g) the turnover component of taxonomic β-diversity, (h–l) functional β-diversity, (m–o) the turnover component of functional β-diversity. The maximum height reached by each function indicates the total amount of β-diversity associated with the gradient of the variable concerned, holding all other variables constant. The slope of each function displays the rate of β-diversity and its variation along the gradient concerned. Up, upstream; up-down, upstream–downstream. The geographic distance unit comes from NMDS coordinates.

13652486, 2023, 7, Downloaded from https://onlinelibrary.wiley.com/doi/10.1111/gcb.16533 by Cochrane France, Wiley Online Library on [06/04/2023]. See the Terms and Conditions (https://onlinelibrary.wiley.com/terms-and-conditions) on Wiley Online Library for rules of use; OA articles are governed by the applicable Creative Commons License

upstream–downstream circular area. This model exhibited similar results to that of the taxonomic β-diversity and explained 74.9% of the total deviance in turnover (Table S10). The most important predictor remained geographic distance with a contribution of 55.3% of the total deviance. The environmental predictor (water temperature) explained 4.7% of the deviance, while the anthropic variable accounted for 4.6% of the deviance (Figure 3c). Taxonomic turnover displayed similar increases to taxonomic β-diversity along the site distance, water temperature and deforestation gradients (Figure 4e–g).

For the functional β-diversity, the GDM with the highest explanatory power was the model considering deforestation over a 30-km upstream sub-basin area. The functional GDM computed with paleo-distances explained 58% of the deviance in β-diversity (Table S10) and showed contrasting results to those revealed by the taxonomic β-diversity and turnover. The major contributors were environmental variables (elevation range, upstream precipitation seasonality and water temperature) accounting together for 21.2% of the deviance. The geographic and anthropic predictors had a low contribution, explaining 6.7% and 4.6% of the deviance, respectively. The shared contribution of environmental and anthropic predictors explained 14.3% of the deviance (Figure 3b). The functional β-diversity did not increase along the entire range of site distances and stabilised between sites exhibiting geographic distances ranging from 50,000 to 1,788,391 NMDS-based distance unit. Similarly, functional β-diversity did not increase along the 0–420 m elevation range gradient and the 25–30°C water temperature gradient. Contrastingly, functional β-diversity steadily increased with upstream precipitation seasonality and deforestation rates (Figure 4h,j,k).

For the functional turnover, the GDM with the highest explanatory power was the model considering deforestation over a 30-km upstream–downstream circular. This model explained 31.6% of the total deviance (Table S10). The anthropic variable was the most important, with a contribution of 16.4% to the total deviance. The geographic predictor was the second most important with 11.8% of the deviance explained, while the most important environmental predictor explained only 1.1% of the deviance (Figure 3d). The functional turnover exhibited the same patterns of variation as functional β-diversity along increasing geographic distances and the deforestation gradient. The pattern of variations along the water temperature gradient was however different, with stabilisation of functional turnover from water temperature ranging from 27.5 to 35°C (Figure 4m–o).

3.3 | Predicting taxonomic and functional fish diversity

The spatialised predictions of taxonomic and functional β-diversity and their turnover component based on geographical, environmental and anthropic variables show how β-diversity varies in space within and between basins in response to each factor (Figure 5).

Spatial predictions of taxonomic and functional β-diversity and turnover based on geography exhibited an east-west gradient (Figure 5a,d,g,j).

Spatial predictions of taxonomic β-diversity in response to environmental variables (elevation range and water temperature) showed that the main course of the Maroni and the Oyapock rivers as well as the Petit Saut Lake contained the fish communities with the highest rate of β-diversity (values approximately ranging from 0.42 to 0.84 GDM-unit, Figure 5b). When only considering taxonomic turnover predictions, similar communities between sections of the Mana, the Kourou, the Comté and the Approuague rivers and the Maroni, Oyapock and Sinnamary rivers are expected (Figure 5e).

Functional β-diversity predictions based on environmental variables (upstream precipitation seasonality, elevation range and water temperature) highlighted similarities not only between communities of the Oyapock and the Maroni courses but also between the inland rivers (Figure 5h). However, when only accounting for functional turnover, almost the entire Maroni, Sinnamary and Oyapock drainages as well as middle sections of the Mana, the Comté and the Approuague rivers exhibited similar communities (Figure 5k).

Predictions of taxonomic β-diversity in response to anthropic activities revealed that the downstream part of the Maroni as well as estuaries of the Comté and the Oyapock rivers displayed the highest rate of β-diversity (summed transformed predictor values were around 0.66, Figure 5c). In comparison, when considering taxonomic turnover predictions, only the middle and downstream course of the Maroni river exhibited the highest rate of β-diversity, (summed transformed predictor values around 0.07, Figure 5f). Spatial predictions of functional β-diversity and turnover were similar to that of taxonomic β-diversity and turnover, respectively (Figure 5c,f,i,l). See Figure S3 for overall predictions of taxonomic and functional β-diversity and its turnover component in response to geographical, environmental and anthropic variables together.

Comparing the similarity between predicted fish communities and WFD survey locations indicates how these survey sites are representative of the regional fish fauna. Overall, the WFD survey sites had a better representation of the fish regional functional diversity (similarity values ranging from 0.48 to 0.76) than taxonomic diversity (similarity values ranging from 0.20 to 0.46) (Figure 6a,b). With fish community predictions based on taxonomic β-diversity, similarity to the WFD survey sites presented variations over the entire hydrographic network with the Kourou, sections of the Sinnamary and the Approuague and the downstream part of the Comté river exhibiting the highest similarities (0.40–0.45). Conversely, upstream sections of the Maroni and the Mana as well as estuaries of the Comté and the Oyapock rivers were less well represented by the WFD survey sites (similarity values ranging between 0.20 and 0.25, Figure 6a). When only considering taxonomic predictions of fish community based on turnover, the overall similarity between regional taxonomic fish diversity and WFD survey sites increased (similarity values ranging from 0.27 to 0.55). This was particularly noticeable in the downstream section of the Maroni and the estuaries of the Oyapock and the Comté rivers (Figure 6c). With fish community predictions based on functional β-diversity predictions, the similarity between regional taxonomic fish diversity and WFD survey sites were high, with similarities to

13652486, 2023, 7, Downloaded from https://onlinelibrary.wiley.com/doi/10.1111/gcb.16533 by Cochrane France, Wiley Online Library on [06/04/2023]. See the Terms and Conditions (https://onlinelibrary.wiley.com/terms-and-conditions) on Wiley Online Library for rules of use; OA articles are governed by the applicable Creative Commons License

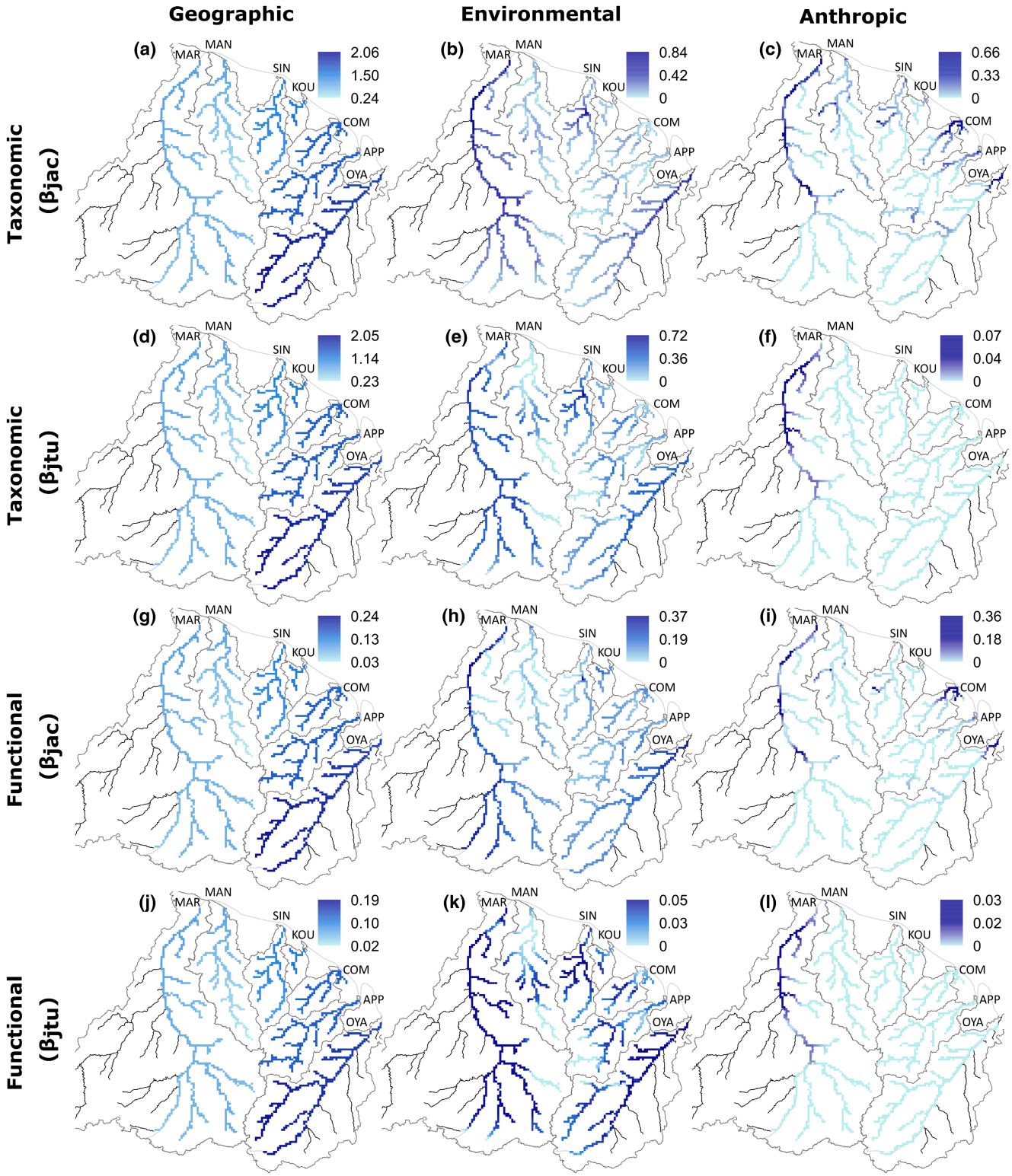

FIGURE 5 Colour maps resulting from the transformed layers of biological relevance presenting the predictions of both overall community dissimilarity (β_{jac}) and its turnover component (β_{jtu}) for taxonomic and functional diversity. Colour maps based on (a,d,g,j) the geographical variable, (b,e,h,k) environmental variables, (c,f,i,l) anthropic variables. Predictions were computed from the best generalized dissimilarity models considering the effect of each factor separately (Table S10). Similar colours depict similarities in assemblages. The colour gradient displays the variation of β-diversity along the geographic, environmental and anthropic gradients. Maroni (MAR), Mana (MAN), Sinnamary (SIN), Kourou (Kou), Comté (COM), Approuague (APP) and Oyapock (OYA). Map lines delineate study areas and do not necessarily depict accepted national boundaries.

13652486, 2023, 7, Downloaded from https://onlinelibrary.wiley.com/doi/10.1111/gcb.16533 by Cochrane France, Wiley Online Library on [06/04/2023]. See the Terms and Conditions (https://onlinelibrary.wiley.com/terms-and-conditions) on Wiley Online Library for rules of use; OA articles are governed by the applicable Creative Commons License

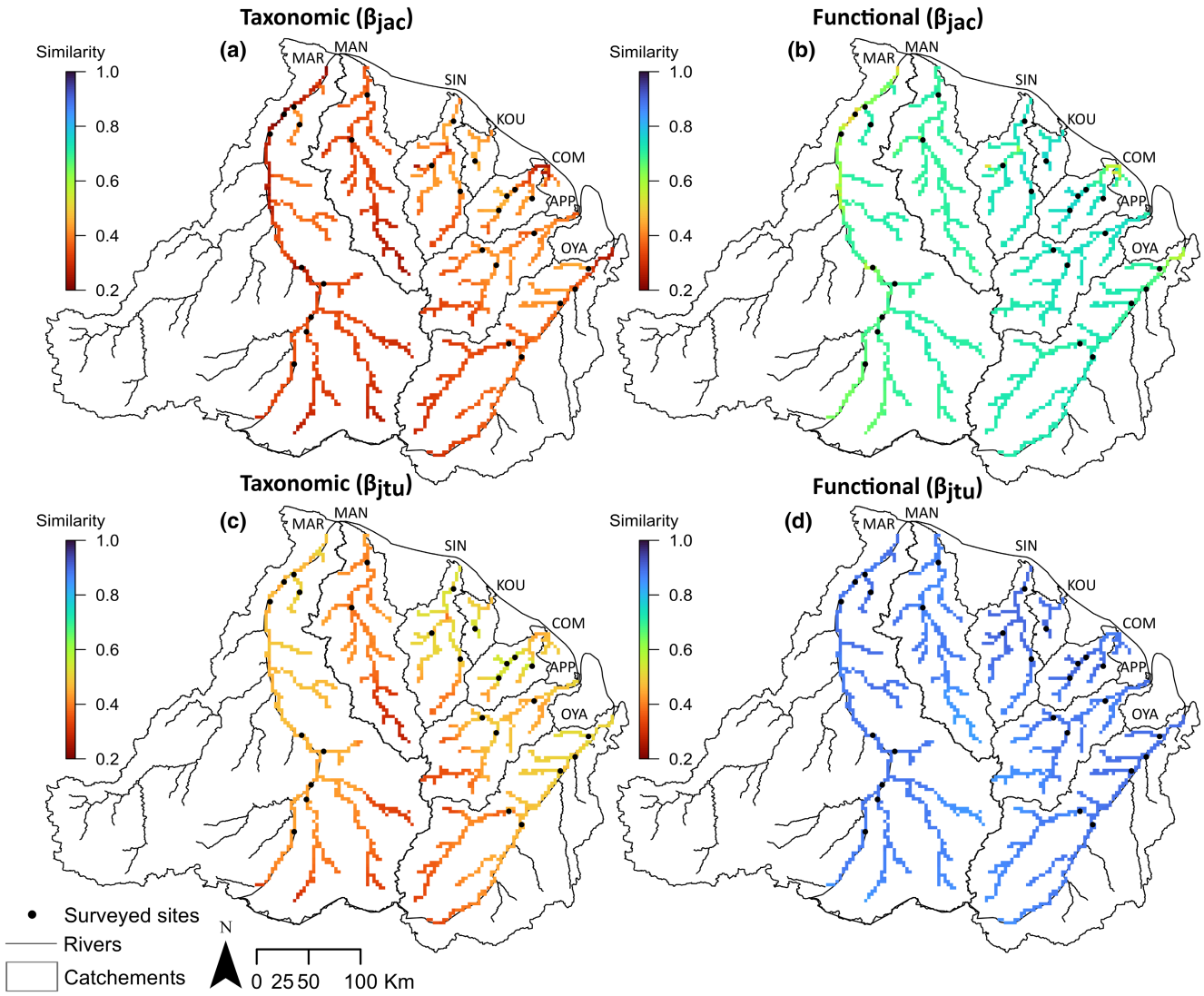

FIGURE 6 Generalized dissimilarity model predictions of β-diversity to assess the representativeness of survey locations. GDM predictions for (a) taxonomic β-diversity, (b) functional β-diversity, (c) the turnover component of taxonomic β-diversity, (d) the turnover component of functional β-diversity. The similarity gradient indicates the mean predicted community similarity of each location (each 1 km-pixel of the hydrographic network) to the 27 survey sites of the EU Water Framework Directive monitoring program (see Section 2). Maroni (MAR), Mana (MAN), Sinnamary (SIN), Kourou (Kou), Comté (COM), Approuague (APP) and Oyapock (OYA). Map lines delineate study areas and do not necessarily depict accepted national boundaries.

the survey sites ranging between 0.70 and 0.76 for most of the hydrographic networks. Only small sections of the Maroni, the Approuague, the Comté and the Oyapock had low similarity to the WFD survey sites, not exceeding 0.6 (range: 0.48–0.60; Figure 6b). When only considering fish community predictions based on functional turnover, the similarity to WFD survey sites increased for the entire river network and exhibited little spatial variations (similarity values ranging from 0.84 to 0.90, Figure 6d).

The comparison of similarity between each location and the entire region revealed unique fish assemblages. With fish community predictions based on taxonomic β-diversity, fish assemblages located downstream in the Maroni and the Comté and Oyapock, estuaries were less similar to the regional taxonomic diversity (similarity values ranging between 0.17 and 0.27, Figure 7a). Contrastingly, considering taxonomic fish community predictions based on turnover, the most unique assemblages were located at the upstream section of the Mana, and on upstream Maroni, Mana, Oyapock and Approuague tributaries (similarity values ranging from 0.31 to 0.37, Figure 7c). Fish community pattern of uniqueness based on functional β-diversity was similar to that of taxonomic β-diversity, while functional turnover exhibited no spatial variation of community uniqueness (Figure 7b,d). The index of uniqueness based on functional diversity nevertheless exhibited a narrower range than that based on taxonomic diversity (similarity values ranging from 0.48 to 0.75 for functional β-diversity and from 0.84 to 0.89 for functional turnover, Figure 7b,d).

13652486, 2023, 7, Downloaded from https://onlinelibrary.wiley.com/doi/10.1111/gcb.16533 by Cochrane France, Wiley Online Library on [06/04/2023]. See the Terms and Conditions (https://onlinelibrary.wiley.com/terms-and-conditions) on Wiley Online Library for rules of use; OA articles are governed by the applicable Creative Commons License

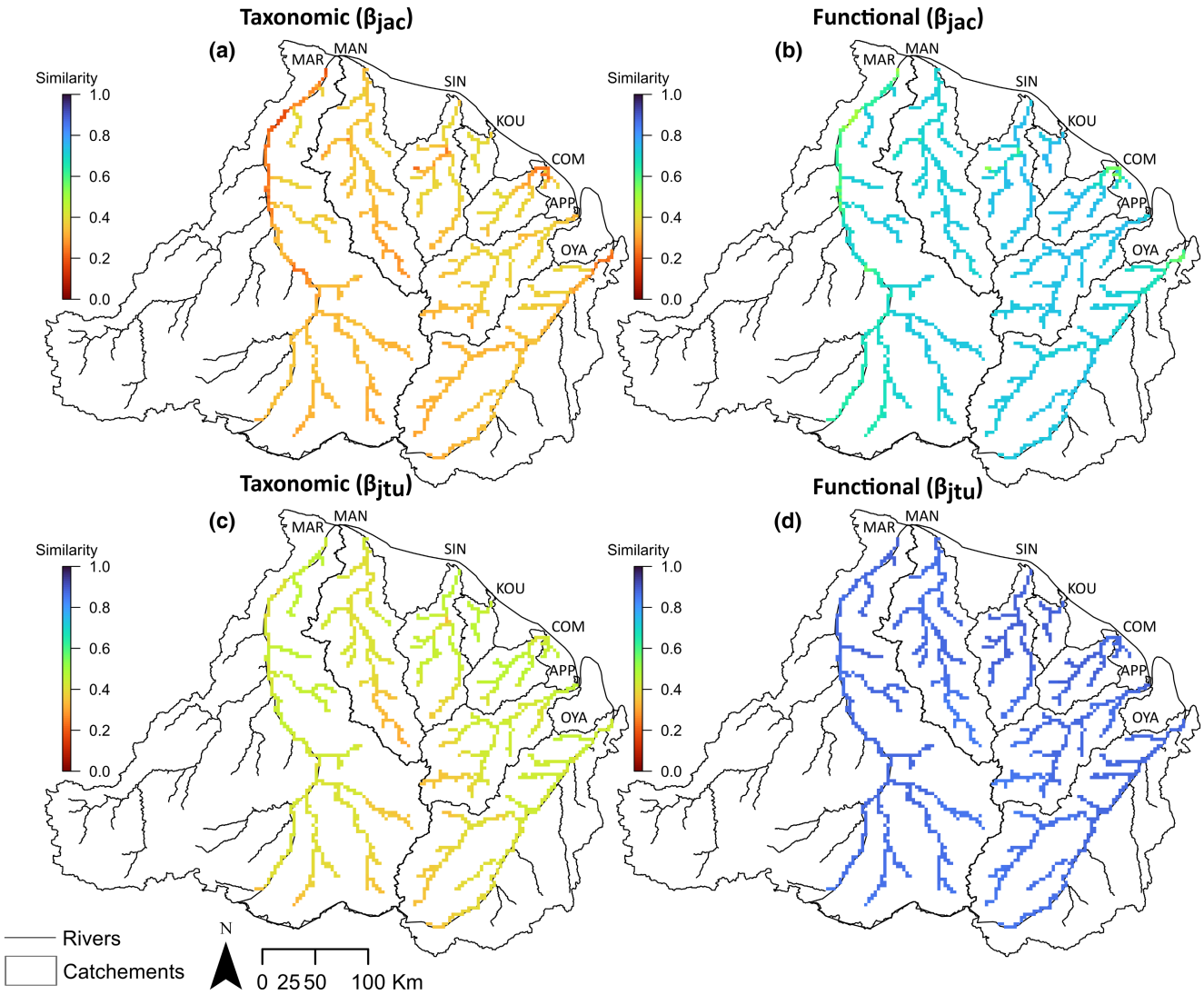

FIGURE 7 Generalized dissimilarity model predictions of β-diversity to assess the uniqueness of each location. GDM predictions for (a) taxonomic β-diversity, (b) functional β-diversity, (c) the turnover component of taxonomic β-diversity, (d) the turnover component of functional β-diversity. The similarity gradient indicates the mean predicted similarity of each location (each 1-km pixel of the hydrographic network) in relation to the entire region. Maroni (MAR), Mana (MAN), Sinnamary (SIN), Kourou (Kou), Comté (COM), Approuague (APP), Oyapock (OYA). Map lines delineate study areas and do not necessarily depict accepted national boundaries.

4 | DISCUSSION

As freshwater ecosystems are organised in network structures following hydrologic pathways (Pringle, 2001), the river connectivity is an important determinant of biodiversity patterns. Thus, management strategies in those ecosystems need to be designed at the catchment scale (IPBES, 2019). However, conservation strategies are often insufficient because it requires knowledge on biodiversity distribution, as well as of their determinants and processes (assembly rules) at the scale of entire basins. This is particularly challenging in Neotropical freshwater regions. These areas concentrate a vast number of species, many of which are rare, and present limited information on species spatial distributions (Mokany et al., 2014). This restricts the suitability of common species-level modelling approaches in depicting information on diversity distribution and its underlying mechanisms (Mokany et al., 2014; Pollock et al., 2020). Here we used community-level modelling, as an efficient alternative to classical species-centred approaches (Pollock et al., 2020) combined with a multifaceted biodiversity approach.

4.1 | Fish assembly rules between and within basins

Multifaceted approaches to biodiversity provide complementary views on the processes that give rise to ecological patterns at different spatial scales (Loiseau et al., 2017). Here, taxonomic and functional β-diversity bring light onto the assembly rules driving

13652486, 2023, 7, Downloaded from https://onlinelibrary.wiley.com/doi/10.1111/gcb.16533 by Cochrane France, Wiley Online Library on [06/04/2023]. See the Terms and Conditions (https://onlinelibrary.wiley.com/terms-and-conditions) on Wiley Online Library for rules of use; OA articles are governed by the applicable Creative Commons License

Neotropical fish communities at both regional and river basin scales. Between basins, our findings revealed mismatching patterns between both facets of fish diversity. The higher taxonomic β-diversity than functional β-diversity indicates that dispersal limitation acts at a higher degree than environmental filtering in shaping fish communities between basins (Benone et al., 2020; Carvajal-Quintero et al., 2019). This is also supported by the taxonomic β-diversity mostly explained by turnover between basins, as species replacement is expected to be higher between localities if species dispersal is limited (García-Navas et al., 2022; Peláez & Pavanelli, 2019). In addition, the high contribution of geographic distance to taxonomic β-diversity and turnover highlighted in the GDMs as well as the increase of the explanatory power of the models when accounting for historical connectivity between basins indicate that dispersal limitation is the major driver of taxonomic fish distribution at the regional scale. It is primarily due to the isolation between river basins by land and seawater, strongly limiting inter-basin dispersal (Dias et al., 2014). Such fish species turnover between drainages gave rise to an East–West similarity gradient of the river drainages, reflecting the historical fluvial connections of the region and the related species dispersal limitation.

Surprisingly, this pattern still holds at the intra-basin level, although the mismatch between the taxonomic and functional β-diversity was less marked. Thus, dispersal limitation still occurs within basins. This process was already reported for fish faunas in small streams, where the main river stem and major tributaries act as barriers against the dispersal of stream species (Cilleros et al., 2016), supporting the general prediction that upstream areas are isolated from each other (Brown & Swan, 2010; Schmera et al., 2018). Here, we show that dispersal limitation still holds for faunas inhabiting large rivers, which contradicts the general theory specifying that large rivers are largely influenced by mass effects (the movement of animals through dispersal) and are, therefore, not constrained by dispersal limitation (Brown & Swan, 2010; Schmera et al., 2018). Such main river dispersal limitation may be due to the natural discontinuities of the fluvial networks (Herrera-Pérez et al., 2019). In the particular case of Guianese fishes, the alternation of slow-flowing areas with rapids and waterfalls, probably explains the observed dispersal limitation within the upstream-downstream course of the rivers.

This has a particular significance for conservation, as faunistic recovery from anthropogenic disturbances may be hampered by dispersal limitation. For instance, dispersal played an important role during the recovery of impacted zooplankton communities (Gray & Arnott, 2011). Naturally discontinued river systems may be even more sensitive to anthropogenic fragmentation, as it can result in a cumulative effect increasing the limitation of species movements along the hydrographic network (Gauthier et al., 2021). It particularly concerns freshwaters ecosystems in the Amazonian region, where the continuous development of dams (Castello & Macedo, 2016) acts as dispersal barriers, disconnecting populations and limiting re-colonisation processes (Winemiller et al., 2016) and, therefore, reducing faunistic recovery in disturbed areas.

4.2 | Anthropic disturbances shape fish diversity

While anthropic activities in this region were shown to drive drastic paired declines of fish taxonomic and functional diversity at the local scale (Cantera, Coutant, et al., 2022), we predicted at the regional scale that functional β-diversity would be more imprinted by anthropic activities than taxonomic β-diversity. We demonstrated that anthropic activities had a weaker contribution than historical and environmental determinants to the taxonomic distribution of fish at the regional scale. Nevertheless, anthropization was here a major determinant of functional β-diversity, resulting in species trait turnover between sites. This mismatch pattern justifies the importance of multifaceted approaches to assess the impact of anthropic activities on biodiversity (Cilleros et al., 2017; Devictor et al., 2010; Jiang et al., 2021; Loiseau et al., 2017). Interestingly, we report a marked shared effect between environmental and anthropic factors in explaining functional β-diversity. Anthropic activities may thus reinforce environmental sorting by modifying environmental parameters through land exploitation and transformation (Roa-Fuentes et al., 2019; Villéger et al., 2010). Although deforestation was used as a proxy for anthropogenic disturbances including gold mining, logging, agriculture and human settlements, gold mining remains the main cause of deforestation in the Northern Amazonian region (Dezécache et al., 2017). Within the studied area, gold mining accounts for more than 40% of the deforested surfaces (Cantera, Coutant, et al., 2022). Gold mining generates both physical and ecotoxicological impacts by releasing pollutants in the water (mercury or cyanide), degrading the riverbed and the banks and altering the water's physicochemistry (Gallay et al., 2018). We already reported that persistent impacts of gold mining throughout the study area drive fish assemblages towards the same local decline in functions, with a loss in small detritivores, invertivores and algae browser fish species (Cantera, Coutant, et al., 2022). Here, the congruent patterns of fish taxonomic and functional β-diversity but also between taxonomic and functional turnover in response to anthropization reflects a biotic homogenization at the anthropized localities. At these localities, the compositional changes within communities result in an increase in similarity between anthropized sites and in a decrease in similarity between disturbed and undisturbed sites. Generally, functional homogenization is the result of the replacement of species with unique functional attributes by functionally redundant species. The loss of functional strategies reflects the vulnerability of the studied ecosystems, altering functional diversity and ecosystem functioning (Clavel et al., 2011).

4.3 | Regional predictions of French-Guianese fish diversity

In this study, using a community-level modelling approach, we illustrated how we can predict taxonomic and functional biodiversity distribution in species-rich environments and unexplored areas. The spatial GDM predictions provided a regional view of

13652486, 2023, 7, Downloaded from https://onlinelibrary.wiley.com/doi/10.1111/gcb.16533 by Cochrane France, Wiley Online Library on [06/04/2023]. See the Terms and Conditions (https://onlinelibrary.wiley.com/terms-and-conditions) on Wiley Online Library for rules of use; OA articles are governed by the applicable Creative Commons License

the spatial variation of fish assemblages based on historical, environmental and anthropic factors. For instance, we predicted the highest rate of β-diversity in response to anthropization in assemblages located in the downstream section of the Maroni river and on the Oyapock and Comté estuaries, as well as on some tributaries of the inland rivers. Predictions based on environmental parameters exhibited contrasting patterns. Taxonomic assemblages of the Maroni and Oyapock rivers were similar but distinct from those of the inland basins. This is possibly due to the length of the two rivers, crossing the entire territory and therefore facing a wider and similar range of environmental variations, notably elevation and water temperature. The assemblage similarity noticeably increased between all basins when only considering functional turnover. This suggests that the inland basins may present differences in the number of functional strategies compared to the Maroni and Oyapock.

Reliable predictions of β-diversity, conditioned upon models' explanatory power and quality, can constitute a basis for biodiversity conservation studies. Mokany et al. (2022) provide a summary of relevant analyses that can be implemented from GDM predictions of β-diversity within the framework of biodiversity conservation studies. For instance, combining the assessment of regional community similarity to focal communities and determining the biodiversity uniqueness of each locality can help identify whether sites surveyed as part of the European WFD monitoring program well represent regional biodiversity.

In general, the predictions demonstrated that functional β-diversity was better represented than taxonomic β-diversity in the WFD survey sites. Interestingly, the communities that were the most poorly represented in terms of functional diversity corresponded to communities exhibiting the highest β-diversity in response to anthropogenic disturbances. These communities were also predicted to be the most unique in terms of functional diversity. Regional functional turnover was well captured in the WFD sites compared with regional taxonomic turnover where the most poorly represented communities were expected to present the most unique taxonomic composition. Our results demonstrate that anthropic disturbances generate assemblages with atypical functional diversity that is poorly captured by the WFD survey sites. These results also indicate that achieving a meaningful taxonomic assessment of the diversity requires the survey of sites distributed all along the hydrographic network. The representativeness of the regional fish diversity in the WFD survey sites could therefore be improved by adding additional localities hosting the most unique assemblages identified here, differing depending on the biodiversity facet.

5 | CONCLUSION

Establishing appropriate conservation strategies to protect freshwater ecosystems at the catchment scale first necessitates disentangling the assembly rules of freshwater communities. This is challenging in species-rich environment because of the lack of knowledge on species distribution. The recent advances in eDNA metabarcoding coupled with adequate biodiversity modelling tools allow the implementation of biodiversity distribution models with high explanatory power that can further be used to project biodiversity at a regional scale. Our study revealed a mismatch between the taxonomic and the functional facet of fish assemblages. While French-Guianese fish taxonomic diversity was mainly structured by dispersal limitation at both intra and inter-basin scales, functional diversity was rather influenced by environmental and anthropic determinants. Importantly, regional predictions of fish biodiversity indicated that survey sites of the EU WFD monitoring program failed to fully capture not only regional taxonomic diversity but also assemblages presenting unique functional diversity in response to human disturbances. This study presents a promising approach to map spatial biodiversity, to design efficient networks of survey sites and to quantify the anthropogenic impact on species-rich environments.

AUTHOR CONTRIBUTIONS

Opale Coutant, Céline Jézéquel, Karel Mokany, Sébastien Brosse and Jérôme Murienne conceived the ideas and designed the methodology; Opale Coutant, Sébastien Brosse and Jérôme Murienne collected the data; Alice Valentini and Tony Dejean supervised the laboratory work and conducted the bioinformatic analyses; Raphaël Covain provided part of genetic material; Opale Coutant analysed the data; Opale Coutant, Céline Jézéquel, Karel Mokany, Sébastien Brosse, Jérôme Murienne and Isabel Cantera led the writing of the manuscript. All authors contributed critically to the manuscript.

ACKNOWLEDGEMENTS

This work benefited from Investissement d'Avenir grants managed by the Agence Nationale de la Recherche (CEBA: ANR-10-LABX-25-01; TULIP: ANR-10-LABX-0041; DRIIHM: ANR-11-LABX-0010), ANR grant (DEBIT: ANR-17-CE02-0007-01). This work is part of the VIGILIFE Sentinel Rivers project. We are indebted to the DGTM Guyane, the 'Office de l'eau' Guyane, the Guiana National Park (PAG), the LEEISA lab, VIGILIFEand HYDRECO for financial and technical support. We also thank SPYGEN staff for the laboratory technical support. Guyane Wild Fish association, including Gregory Quartarollo and Hadrien Lalagüe provided part of the fish pictures for morphological measures.

CONFLICT OF INTEREST

Teleo primers and the use of the amplified fragment for identifying fish species from environmental samples are patented by the CNRS and the Université Grenoble Alpes. This patent only restricts commercial applications and has no implications for the use of this method by academic researchers. SPYGEN owns a license for this patent. AV and TD are research scientists at a private company specializing in the use of eDNA for species detection (SPYGEN).

DATA AVAILABILITY STATEMENT

Supplementary materials including Figures S1 to S3 and Tables S1 to S10 underlying the main results of the study are provided in the online

13652486, 2023, 7, Downloaded from https://onlinelibrary.wiley.com/doi/10.1111/gcb.16533 by Cochrane France, Wiley Online Library on [06/04/2023]. See the Terms and Conditions (https://onlinelibrary.wiley.com/terms-and-conditions) on Wiley Online Library for rules of use; OA articles are governed by the applicable Creative Commons License

version of the article. For the sites on the Sinnamary river, the data that support the findings (raw sequences) of this study are openly available in "figshare" at https://doi.org/10.6084/m9.figshare.13739086.v7 using the Metadata_Sinnamary_Fish file to link "Site name" and "PCR sample". For the sites on the Maroni and Oyapock rivers, the data that support the findings (raw sequences) of this study are openly available in "Dryad" at https://doi.org/10.5061/dryad.pvmcvdnmr using the file "Squencing_infos" to link "Site name" and "PCR sample".

ORCID

Opale Coutant https://orcid.org/0000-0003-4170-6264
Céline Jézéquel https://orcid.org/0000-0003-0687-1467
Karel Mokany https://orcid.org/0000-0003-4199-3697
Isabel Cantera https://orcid.org/0000-0003-3161-1878
Raphaël Covain https://orcid.org/0000-0002-8186-8914
Alice Valentini https://orcid.org/0000-0001-5829-5479
Tony Dejean https://orcid.org/0000-0002-5115-4902
Sébastien Brosse https://orcid.org/0000-0002-3659-8177
Jérôme Murienne https://orcid.org/0000-0003-1474-7829

REFERENCES

Albert, J. S., Destouni, G., Duke-Sylvester, S. M., Magurran, A. E., Oberdorff, T., Reis, R. E., Winemiller, K. O., & Ripple, W. J. (2021). Scientists' warning to humanity on the freshwater biodiversity crisis. *Ambio*, *50*(1), 85–94. https://doi.org/10.1007/s13280-020-01318-8

Baselga, A. (2010). Partitioning the turnover and nestedness components of beta diversity. *Global Ecology and Biogeography*, *19*(1), 134–143. https://doi.org/10.1111/j.1466-8238.2009.00490.x

Baselga, A., & Orme, C. D. L. (2012). Betapart: An R package for the study of beta diversity. *Methods in Ecology and Evolution*, *3*(5), 808–812. https://doi.org/10.1111/j.2041-210X.2012.00224.x

Becker, J. J., Sandwell, D. T., Smith, W. H. F., Braud, J., Binder, B., Depner, J., Fabre, D., Factor, J., Ingalls, S., Kim, S.-H., Ladner, R., Marks, K., Nelson, S., Pharaoh, A., Trimmer, R., von Rosenberg, J., Wallace, G., & Weatherall, P. (2009). Global bathymetry and elevation data at 30 arc seconds resolution: SRTM30_PLUS. *Marine Geodesy*, *32*(4), 355–371 https://topex.ucsd.edu/WWW_html/srtm30_plus.html

Benone, N. L., Leal, C. G., dos Santos, L. L., Mendes, T. P., Heino, J., & de Assis Montag, L. F. (2020). Unravelling patterns of taxonomic and functional diversity of Amazon stream fish. *Aquatic Sciences*, *82*(4), 1–11. https://doi.org/10.1007/s00027-020-00749-5

Biggs, J., Ewald, N., Valentini, A., Gaboriaud, C., Dejean, T., Griffiths, R. A., Foster, J., Wilkinson, J. W., Arnell, A., Brotherton, P., Williams, P., & Dunn, F. (2015). Using eDNA to develop a national citizen science-based monitoring programme for the great crested newt (*Triturus cristatus*). *Biological Conservation*, *183*, 19–28. https://doi.org/10.1016/j.biocon.2014.11.029

Blackman, R. C., Osathanunkul, M., Brantschen, J., di Muri, C., Harper, L. R., Mächler, E., Hänfling, B., & Altermatt, F. (2021). Mapping biodiversity hotspots of fish communities in subtropical streams through environmental DNA. *Scientific Reports*, *11*(1), 10375. https://doi.org/10.1038/s41598-021-89942-6

Boyer, F., Mercier, C., Bonin, A., Le Bras, Y., Taberlet, P., & Coissac, E. (2016). obitools: A unix-inspired software package for DNA metabarcoding. *Molecular Ecology Resources*, *16*(1), 176–182. https://doi.org/10.1111/1755-0998.12428

Brown, B. L., & Swan, C. M. (2010). Dendritic network structure constrains metacommunity properties in riverine ecosystems. *Journal of Animal Ecology*, *79*(3), 571–580. https://doi.org/10.1111/j.1365-2656.2010.01668.x

Cailliez, F. (1983). The analytical solution of the additive constant problem. *Psychometrika*, *48*(2), 305–308. https://doi.org/10.1007/BF02294026

Cantera, I., Cilleros, K., Valentini, A., Cerdan, A., Dejean, T., Iribar, A., Taberlet, P., Vigouroux, R., & Brosse, S. (2019). Optimizing environmental DNA sampling effort for fish inventories in tropical streams and rivers. *Scientific Reports*, *9*(1), 1–11. https://doi.org/10.1038/s41598-019-39399-5

Cantera, I., Coutant, O., Jézéquel, C., Decotte, J.-B., Dejean, T., Iribar, A., Vigouroux, R., Valentini, A., Murienne, J., & Brosse, S. (2022). Low level of anthropization linked to harsh vertebrate biodiversity declines in Amazonia. *Nature Communications*, *13*(1), 3290. https://doi.org/10.1038/s41467-022-30842-2

Cantera, I., Decotte, J., Dejean, T., Murienne, J., Vigouroux, R., Valentini, A., & Brosse, S. (2022). Characterizing the spatial signal of environmental DNA in river systems using a community ecology approach. *Molecular Ecology Resources*, *22*(4), 1274–1283. https://doi.org/10.1111/1755-0998.13544

Carraro, L., Mächler, E., Wüthrich, R., & Altermatt, F. (2020). Environmental DNA allows upscaling spatial patterns of biodiversity in freshwater ecosystems. *Nature Communications*, *11*(1), 1–12. https://doi.org/10.1038/s41467-020-17337-8

Carvajal-Quintero, J., Villalobos, F., Oberdorff, T., Grenouillet, G., Brosse, S., Hugueny, B., Jézéquel, C., & Tedesco, P. A. (2019). Drainage network position and historical connectivity explain global patterns in freshwater fishes' range size. *Proceedings of the National Academy of Sciences of the United States of America*, *116*(27), 13434–13439. https://doi.org/10.1073/pnas.1902484116

Carvalho, J. C., Cardoso, P., & Gomes, P. (2012). Determining the relative roles of species replacement and species richness differences in generating beta-diversity patterns. *Global Ecology and Biogeography*, *21*(7), 760–771. https://doi.org/10.1111/j.1466-8238.2011.00694.x

Castello, L., & Macedo, M. N. (2016). Large-scale degradation of Amazonian freshwater ecosystems. *Global Change Biology*, *22*(3), 990–1007. https://doi.org/10.1111/gcb.13173

Castello, L., Mcgrath, D. G., Hess, L. L., Coe, M. T., Lefebvre, P. A., Petry, P., Macedo, M. N., Renó, V. F., & Arantes, C. C. (2013). The vulnerability of Amazon freshwater ecosystems. *Conservation Letters*, *6*(4), 217–229. https://doi.org/10.1111/conl.12008

Cilleros, K., Allard, L., Grenouillet, G., & Brosse, S. (2016). Taxonomic and functional diversity patterns reveal different processes shaping European and Amazonian stream fish assemblages. *Journal of Biogeography*, *43*(9), 1832–1843. https://doi.org/10.1111/jbi.12839

Cilleros, K., Allard, L., Vigouroux, R., & Brosse, S. (2017). Disentangling spatial and environmental determinants of fish species richness and assemblage structure in Neotropical rainforest streams. *Freshwater Biology*, *62*(10), 1707–1720. https://doi.org/10.1111/fwb.12981

Cilleros, K., Valentini, A., Allard, L., Dejean, T., Etienne, R., Grenouillet, G., Iribar, A., Taberlet, P., Vigouroux, R., & Brosse, S. (2019). Unlocking biodiversity and conservation studies in high-diversity environments using environmental DNA (eDNA): A test with Guianese freshwater fishes. *Molecular Ecology Resources*, *19*(1), 27–46. https://doi.org/10.1111/1755-0998.12900

Clavel, J., Julliard, R., & Devictor, V. (2011). Worldwide decline of specialist species: Toward a global functional homogenization? *Frontiers in Ecology and the Environment*, *9*(4), 222–228. https://doi.org/10.1890/080216

Coutant, O., Cantera, I., Cilleros, K., Dejean, T., Valentini, A., Murienne, J., & Brosse, S. (2020, June). Detecting fish assemblages with environmental DNA: Does protocol matter? Testing eDNA metabarcoding

13652486, 2023, 7, Downloaded from https://onlinelibrary.wiley.com/doi/10.1111/gcb.16533 by Cochrane France, Wiley Online Library on [06/04/2023]. See the Terms and Conditions (https://onlinelibrary.wiley.com/terms-and-conditions) on Wiley Online Library for rules of use; OA articles are governed by the applicable Creative Commons License

method robustness. *Environmental DNA*, *3*(3), 619–630. https://doi.org/10.1002/edn3.158

De Barba, M., Miquel, C., Boyer, F., Mercier, C., Rioux, D., Coissac, E., & Taberlet, P. (2014). DNA metabarcoding multiplexing and validation of data accuracy for diet assessment: Application to omnivorous diet. *Molecular Ecology Resources*, *14*(2), 306–323. https://doi.org/10.1111/1755-0998.12188

Devictor, V., Mouillot, D., Meynard, C., Jiguet, F., Thuiller, W., & Mouquet, N. (2010). Spatial mismatch and congruence between taxonomic, phylogenetic and functional diversity: The need for integrative conservation strategies in a changing world. *Ecology Letters*, *13*(8), 1030–1040. https://doi.org/10.1111/j.1461-0248.2010.01493.x

Dezécache, C., Faure, E., Gond, V., Salles, J. M., Vieilledent, G., & Hérault, B. (2017). Gold-rush in a forested El Dorado: Deforestation leakages and the need for regional cooperation. *Environmental Research Letters*, *12*(3), 034013. https://doi.org/10.1088/1748-9326/aa6082

Dias, M. S., Oberdorff, T., Hugueny, B., Leprieur, F., Jézéquel, C., Cornu, J. F., Brosse, S., Grenouillet, G., & Tedesco, P. A. (2014). Global imprint of historical connectivity on freshwater fish biodiversity. *Ecology Letters*, *17*(9), 1130–1140. https://doi.org/10.1111/ele.12319

Dickie, I. A., Boyer, S., Buckley, H. L., Duncan, R. P., Gardner, P. P., Hogg, I. D., Holdaway, R. J., Lear, G., Makiola, A., Morales, S. E., Powell, J. R., & Weaver, L. (2018). Towards robust and repeatable sampling methods in eDNA-based studies. *Molecular Ecology Resources*, *18*(5), 940–952. https://doi.org/10.1111/1755-0998.12907

Domisch, S., Amatulli, G., & Jetz, W. (2015). Near-global freshwater-specific environmental variables for biodiversity analyses in 1 km resolution. *Scientific Data*, *2*(1), 1–13. https://doi.org/10.1038/sdata.2015.73

Dudgeon, D., Arthington, A. H., Gessner, M. O., Kawabata, Z. I., Knowler, D. J., Lévêque, C., Naiman, R. J., Prieur-Richard, A. H., Soto, D., Stiassny, M. L. J., & Sullivan, C. A. (2006). Freshwater biodiversity: Importance, threats, status and conservation challenges. *Biological Reviews of the Cambridge Philosophical Society*, *81*(2), 163–182. https://doi.org/10.1017/S1464793105006950

Ferrier, S., Manion, G., Elith, J., & Richardson, K. (2007). Using generalized dissimilarity modelling to analyse and predict patterns of beta diversity in regional biodiversity assessment. *Diversity and Distributions*, *13*(3), 252–264. https://doi.org/10.1111/j.1472-4642.2007.00341.x

Fitzpatrick, M., Mokany, K., Manion, G., Nieto-Lugilde, D., & Ferrier, S. (2022). *gdm: generalized dissimilarity modeling*. Article R package version 1.5.

Gallay, M., Martinez, J. M., Allo, S., Mora, A., Cochonneau, G., Gardel, A., Doudou, J. C., Sarrazin, M., Chow-Toun, F., & Laraque, A. (2018). Impact of land degradation from mining activities on the sediment fluxes in two large rivers of French Guiana. *Land Degradation and Development*, *29*(12), 4323–4336. https://doi.org/10.1002/ldr.3150

García-Navas, V., Martínez-Núñez, C., Tarifa, R., Molina-Pardo, J. L., Valera, F., Salido, T., Camacho, F. M., & Rey, P. J. (2022). Partitioning beta diversity to untangle mechanisms underlying the assembly of bird communities in Mediterranean olive groves. *Diversity and Distributions*, *28*(1), 112–127. https://doi.org/10.1111/ddi.13445

Gauthier, M., le Goff, G., Launay, B., Douady, C. J., & Datry, T. (2021). Dispersal limitation by structures is more important than intermittent drying effects for metacommunity dynamics in a highly fragmented river network. *Freshwater Science*, *40*(2), 302–315. https://doi.org/10.1086/714376

Gray, D. K., & Arnott, S. E. (2011). Does dispersal limitation impact the recovery of zooplankton communities damaged by a regional stressor? *Ecological Applications*, *21*(4), 1241–1256. https://doi.org/10.1890/10-0364.1

Hansen, M. C., Potapov, P. V., Moore, R., Hancher, M., Turubanova, S. A., Tyukavina, A., Thau, D., Stehman, S. V., Goetz, S. J., Loveland, T. R., Kommareddy, A., Egorov, A., Chini, L., Justice, C. O., & Townshend, J. R. G. (2013). High-resolution global maps of 21st-century forest cover change. *Science*, *342*, 850–853. https://doi.org/10.1126/science.1244693

Harvey, E., Gounand, I., Fronhofer, E. A., & Altermatt, F. (2018). Disturbance reverses classic biodiversity predictions in river-like landscapes. *Proceedings of the Royal Society B: Biological Sciences*, *285*(1893), 20182441. https://doi.org/10.1098/rspb.2018.2441

Herrera-Pérez, J., Parra, J. L., Restrepo-Santamaría, D., & Jiménez-Segura, L. F. (2019). The influence of abiotic environment and connectivity on the distribution of diversity in an Andean fish fluvial network. *Frontiers in Environmental Science*, *7*(FEB), 1–8. https://doi.org/10.3389/fenvs.2019.00009

INSEE. (2020). Population légales 2017. https://www.insee.fr/

IPBES. (2019). Global assessment report on biodiversity and ecosystem services of the Intergovernmental Science-Policy Platform on Biodiversity and Ecosystem Services. https://doi.org/10.5281/ZENODO.6417333

Jiang, X., Pan, B., Jiang, W., Hou, Y., Yang, H., Zhu, P., & Heino, J. (2021). The role of environmental conditions, climatic factors and spatial processes in driving multiple facets of stream macroinvertebrate beta diversity in a climatically heterogeneous mountain region. *Ecological Indicators*, *124*, 107407. https://doi.org/10.1016/j.ecolind.2021.107407

Lear, G., Dickie, I., Banks, J., Boyer, S., Buckley, H., Buckley, T., Cruickshank, R., Dopheide, A., Handley, K., Hermans, S., Kamke, J., Lee, C., MacDiarmid, R., Morales, S., Orlovich, D., Smissen, R., Wood, J., & Holdaway, R. (2018). Methods for the extraction, storage, amplification and sequencing of DNA from environmental samples. *New Zealand Journal of Ecology*, *42*(1), 10. https://doi.org/10.20417/nzjecol.42.9

Loiseau, N., Legras, G., Kulbicki, M., Mérigot, B., Harmelin-Vivien, M., Mazouni, N., Galzin, R., & Gaertner, J. C. (2017). Multi-component β-diversity approach reveals conservation dilemma between species and functions of coral reef fishes. *Journal of Biogeography*, *44*(3), 537–547. https://doi.org/10.1111/jbi.12844

López-Delgado, E. O., Winemiller, K. O., & Villa-Navarro, F. A. (2020). Local environmental factors influence beta-diversity patterns of tropical fish assemblages more than spatial factors. *Ecology*, *101*(2), e02940. https://doi.org/10.1002/ecy.2940

Maire, E., Grenouillet, G., Brosse, S., & Villéger, S. (2015). How many dimensions are needed to accurately assess functional diversity? A pragmatic approach for assessing the quality of functional spaces. *Global Ecology and Biogeography*, *24*(6), 728–740. https://doi.org/10.1111/geb.12299

Mokany, K., Ware, C., Woolley, S. N. C., Ferrier, S., & Fitzpatrick, M. C. (2022). A working guide to harnessing generalized dissimilarity modelling for biodiversity analysis and conservation assessment. *Global Ecology and Biogeography*, *31*(4), 802–821. https://doi.org/10.1111/geb.13459

Mokany, K., Westcott, D. A., Prasad, S., Ford, A. J., & Metcalfe, D. J. (2014). Identifying priority areas for conservation and management in diverse tropical forests. *PLoS ONE*, *9*(2), e89084. https://doi.org/10.1371/journal.pone.0089084

Murienne, J., Cantera, I., Cerdan, A., Cilleros, K., Decotte, J.-B., Dejean, T., Vigouroux, R., & Brosse, S. (2019). Aquatic eDNA for monitoring French Guiana biodiversity. *Biodiversity Data Journal*, *7*, e37518. https://doi.org/10.3897/bdj.7.e37518

Naimi, B. (2015). *usdm: Uncertainty analysis for species distribution models*. R package version 1.1-18. https://cran.r-project.org/web/packages/usdm/index.html (No. 1, 1–12; pp. 1–12). https://www.researchgate.net/publication/303174794_Usdm_Uncertainty_analysis_for_species_distribution_models

Peláez, O., & Pavanelli, C. S. (2019). Environmental heterogeneity and dispersal limitation explain different aspects of β-diversity in Neotropical fish assemblages. *Freshwater Biology*, *64*(3), 497–505. https://doi.org/10.1111/fwb.13237

13652486, 2023, 7, Downloaded from https://onlinelibrary.wiley.com/doi/10.1111/gcb.16533 by Cochrane France, Wiley Online Library on [06/04/2023]. See the Terms and Conditions (https://onlinelibrary.wiley.com/terms-and-conditions) on Wiley Online Library for rules of use; OA articles are governed by the applicable Creative Commons License

Polanco, F. A., Richards, E., Flück, B., Valentini, A., Altermatt, F., Brosse, S., Walser, J.-C., Eme, D., Marques, V., Manel, S., Albouy, C., Dejean, T., & Pellissier, L. (2021). Comparing the performance of 12S mitochondrial primers for fish environmental DNA across ecosystems. *Environmental DNA*, *3*(6), 1113–1127. https://doi.org/10.1002/edn3.232

Pollock, L. J., O'Connor, L. M. J., Mokany, K., Rosauer, D. F., Talluto, M. V., & Thuiller, W. (2020). Protecting biodiversity (in all its complexity): New models and methods. *Trends in Ecology & Evolution*, *35*(12), 1119–1128. https://doi.org/10.1016/j.tree.2020.08.015

Pringle, C. M. (2001). Hydrologic connectivity and the management of biological reserves: A global perspective. *Ecological Applications*, *11*(4), 981–998. https://doi.org/10.1890/1051-0761(2001)011[0981:HCATMO]2.0.CO;2

Qian, H., Ricklefs, R. E., & White, P. S. (2005). Beta diversity of angiosperms in temperate floras of eastern Asia and eastern North America. *Ecology Letters*, *8*(1), 15–22. https://doi.org/10.1111/j.1461-0248.2004.00682.x

Rahm, M., Thibault, P., Shapiro, A., Smartt, T., Paloeng, C., Crabbe, S., Farias, P., Carvalho, R., Joubert, P., Rampersaud, P., Pinas, J., Oliveira, M., & Vallauri, D. (2017). Monitoring the impact of gold mining on the forest cover and freshwater in the Guiana Shield Reviewers: Hausil F.

Roa-Fuentes, C. A., Heino, J., Cianciaruso, M. v., Ferraz, S., Zeni, J. O., & Casatti, L. (2019). Taxonomic, functional, and phylogenetic β-diversity patterns of stream fish assemblages in tropical agroecosystems. *Freshwater Biology*, *64*(3), 447–460. https://doi.org/10.1111/fwb.13233

Schmera, D., Árva, D., Boda, P., Bódis, E., Bolgovics, Á., Borics, G., Csercsa, A., Deák, C., Krasznai, E., Lukács, B. A., Mauchart, P., Móra, A., Sály, P., Specziár, A., Süveges, K., Szivák, I., Takács, P., Tóth, M., Várbíró, G., … Erős, T. (2018). Does isolation influence the relative role of environmental and dispersal-related processes in stream networks? An empirical test of the network position hypothesis using multiple taxa. *Freshwater Biology*, *63*(1), 74–85. https://doi.org/10.1111/fwb.12973

Schnell, I. B., Bohmann, K., & Gilbert, M. T. P. (2015). Tag jumps illuminated—Reducing sequence-to-sample misidentifications in metabarcoding studies. *Molecular Ecology Resources*, *15*(6), 1289–1303. https://doi.org/10.1111/1755-0998.12402

Shu, L., Ludwig, A., & Peng, Z. (2020). Standards for methods utilizing environmental DNA for detection of fish species. *Genes*, *11*(3), 296. https://doi.org/10.3390/genes11030296

Socolar, J. B., Gilroy, J. J., Kunin, W. E., & Edwards, D. P. (2016). How should beta-diversity inform biodiversity conservation? *Trends in Ecology & Evolution*, *31*(1), 67–80. https://doi.org/10.1016/j.tree.2015.11.005

Su, G., Logez, M., Xu, J., Tao, S., Villéger, S., & Brosse, S. (2021). Human impacts on global freshwater fish biodiversity. *Science*, *371*(6531), 835–838. https://doi.org/10.1126/science.abd3369

Taberlet, P., Bonin, A., Zinger, L., & Coissac, E. (2018). *Environmental DNA: For biodiversity research and monitoring*. Oxford University Press. https://doi.org/10.1093/oso/9780198767220.001.0001

Taberlet, P., Coissac, E., Pompanon, F., Brochmann, C., & Willerslev, E. (2012). Towards next-generation biodiversity assessment using DNA metabarcoding. *Molecular Ecology*, *21*(8), 2045–2050. https://doi.org/10.1111/j.1365-294X.2012.05470.x

Valentini, A., Taberlet, P., Miaud, C., Civade, R., Herder, J., Thomsen, P. F., Bellemain, E., Besnard, A., Coissac, E., Boyer, F., Gaboriaud, C., Jean, P., Poulet, N., Roset, N., Copp, G. H., Geniez, P., Pont, D., Argillier, C., Baudoin, J. M., … Dejean, T. (2016). Next-generation monitoring of aquatic biodiversity using environmental DNA metabarcoding. *Molecular Ecology*, *25*(4), 929–942. https://doi.org/10.1111/mec.13428

van der Laan, R. (2020). Freshwater fish list. (Vol. 30). https://www.researchgate.net/publication/343920946_Freshwater_Fish_List_30th_ed_Sept_2020

Vannote, R. L., Minshall, G. W., Cummins, K. W., Sedell, J. R., & Cushing, C. E. (1980). The river continuum concept. *Canadian Journal of Fisheries and Aquatic Sciences*, *37*(1), 130–137. https://doi.org/10.1139/f80-017

van Rees, C. B., Waylen, K. A., Schmidt-Kloiber, A., Thackeray, S. J., Kalinkat, G., Martens, K., Domisch, S., Lillebø, A. I., Hermoso, V., Grossart, H. P., Schinegger, R., Decleer, K., Adriaens, T., Denys, L., Jarić, I., Janse, J. H., Monaghan, M. T., de Wever, A., Geijzendorffer, I., … Jähnig, S. C. (2021). Safeguarding freshwater life beyond 2020: Recommendations for the new global biodiversity framework from the European experience. *Conservation Letters*, *14*(1), e12771. https://doi.org/10.1111/conl.12771

Vié, J. C. (1999). Wildlife rescues—The case of the Petit Saut hydroelectric dam in French Guiana. *Oryx*, *33*(2), 115–126. https://doi.org/10.1046/j.1365-3008.1999.00037.x

Villéger, S., Brosse, S., Mouchet, M., Mouillot, D., & Vanni, M. J. (2017). Functional ecology of fish: Current approaches and future challenges. *Aquatic Sciences*, *79*(4), 783–801. https://doi.org/10.1007/s00027-017-0546-z

Villéger, S., Grenouillet, G., & Brosse, S. (2013). Decomposing functional β-diversity reveals that low functional β-diversity is driven by low functional turnover in European fish assemblages. *Global Ecology and Biogeography*, *22*(6), 671–681. https://doi.org/10.1111/geb.12021

Villéger, S., Miranda, J. R., Hernández, D. F., & Mouillot, D. (2010). Contrasting changes in taxonomic vs. functional diversity of tropical fish communities after habitat degradation. *Ecological Applications*, *20*(6), 1512–1522. https://doi.org/10.1890/09-1310.1

Whittaker, R. H. (1960). Vegetation of the Siskiyou Mountains, Oregon and California. *Ecological Monograph*, *30*(3), 279–338.

Winemiller, K. O., McIntyre, P. B., Castello, L., Fluet-Chouinard, E., Giarrizzo, T., Nam, S., Baird, I. G., Darwall, W., Lujan, N. K., Harrison, I., Stiassny, M. L. J., Silvano, R. A. M., Fitzgerald, D. B., Pelicice, F. M., Agostinho, A. A., Gomes, L. C., Albert, J. S., Baran, E., Petrere, M., … Sáenz, L. (2016). Balancing hydropower and biodiversity in the Amazon, Congo, and Mekong. *Science*, *351*(6269), 128–129. https://doi.org/10.1126/science.aac7082

Zeni, J. O., Pérez-Mayorga, M. A., Roa-Fuentes, C. A., Brejão, G. L., & Casatti, L. (2019). How deforestation drives stream habitat changes and the functional structure of fish assemblages in different tropical regions. *Aquatic Conservation: Marine and Freshwater Ecosystems*, *29*(8), 1238–1252. https://doi.org/10.1002/aqc.3128

SUPPORTING INFORMATION

Additional supporting information can be found online in the Supporting Information section at the end of this article.

How to cite this article: Coutant, O., Jézéquel, C., Mokany, K., Cantera, I., Covain, R., Valentini, A., Dejean, T., Brosse, S., & Murienne, J. (2023). Environmental DNA reveals a mismatch between diversity facets of Amazonian fishes in response to contrasting geographical, environmental and anthropogenic effects. *Global Change Biology*, *29*, 1741–1758. https://doi.org/10.1111/gcb.16533

13652486, 2023, 7, Downloaded from https://onlinelibrary.wiley.com/doi/10.1111/gcb.16533 by Cochrane France, Wiley Online Library on [06/04/2023]. See the Terms and Conditions (https://onlinelibrary.wiley.com/terms-and-conditions) on Wiley Online Library for rules of use; OA articles are governed by the applicable Creative Commons License